

Towards a holographic dual of large- N_c QCD

Martín Kruczenski,^a David Mateos,^b Robert C. Myers^{b,c} and David J. Winters^{b,d}

^a *Department of Physics, Brandeis University
Waltham, MA 02454, USA*

^b *Perimeter Institute for Theoretical Physics
Waterloo, Ontario N2J 2W9, Canada*

^c *Department of Physics, University of Waterloo
Waterloo, Ontario N2L 3G1, Canada*

^d *Department of Physics, McGill University
Montréal, Québec H3A 2T8, Canada*

*E-mail: martink@brandeis.edu, dmateos@perimeterinstitute.ca,
rmyers@perimeterinstitute.ca, winters@physics.mcgill.ca*

ABSTRACT: We study N_f D6-brane probes in the supergravity background dual to N_c D4-branes compactified on a circle with supersymmetry-breaking boundary conditions. In the limit in which the resulting Kaluza–Klein modes decouple, the gauge theory reduces to non-supersymmetric, four-dimensional QCD with N_c colours and $N_f \ll N_c$ flavours. As expected, this decoupling is not fully realised within the supergravity/Born–Infeld approximation. For $N_f = 1$ and massless quarks, $m_q = 0$, we exhibit spontaneous chiral symmetry breaking by a quark condensate, $\langle \bar{\psi}\psi \rangle \neq 0$, and find the associated massless ‘pion’ in the spectrum. The latter becomes massive for $m_q > 0$, obeying the Gell–Mann–Oakes–Renner relation: $M_\pi^2 = -m_q \langle \bar{\psi}\psi \rangle / f_\pi^2$. In the case $N_f > 1$ we provide a holographic version of the Vafa–Witten theorem, which states that the $U(N_f)$ flavour symmetry cannot be spontaneously broken. Further, we find $N_f^2 - 1$ unexpectedly light pseudo-scalar mesons in the spectrum. We argue that these are not (pseudo-)Goldstone bosons and speculate on the string mechanism responsible for their lightness. We then study the theory at finite temperature and exhibit a phase transition associated with a discontinuity in $\langle \bar{\psi}\psi \rangle(T)$. D6/ $\overline{D6}$ pairs are also briefly discussed.

KEYWORDS: D-branes, Supersymmetry and Duality.

Contents

1. Introduction and summary of results	1
2. Chiral symmetry breaking from D6-brane embeddings	4
2.1 The D4-soliton background	5
2.2 D6-brane embeddings	7
3. Meson spectroscopy from D6-brane fluctuations ($N_f = 1$)	13
3.1 Analysis of the spectrum	14
3.2 Stability Issues	19
4. The pseudo-Goldstone boson	21
5. Multiple flavours ($N_f > 1$) and a holographic Vafa–Witten theorem	24
6. Finite temperature physics	28
7. D4/D6/$\overline{\text{D6}}$-intersections	34
8. Discussion	37

1. Introduction and summary of results

The AdS₅/CFT₄ correspondence relates string theory on the near-horizon background of N_c D3-branes to the conformal field theory living on their worldvolume [1]. Inspired by this correspondence, Witten proposed a construction of the holographic dual of four-dimensional, pure $SU(N_c)$ Yang–Mills (YM) theory [2]. One starts with N_c D4-branes compactified on a circle of radius M_{KK}^{-1} , and further imposes anti-periodic boundary conditions for the worldvolume fermions on this circle. Before compactification, the D4-brane theory is a five-dimensional, supersymmetric $SU(N_c)$ gauge theory whose field content includes fermions and scalars in the adjoint representation of $SU(N_c)$, in addition to the gauge fields. At energies much below the compactification scale, M_{KK} , the theory is effectively four-dimensional. The anti-periodic boundary conditions break all of the supersymmetries and give a tree-level mass to the fermions, while the scalars also acquire a mass through one loop-effects. Thus at sufficiently low energies the dynamics is that of four-dimensional, massless gluons.

The D4-brane system above has a dual description in terms of string theory in the near-horizon region of the associated (non-supersymmetric) supergravity background. Unfortunately, as observed in [2], the Kaluza–Klein (KK) modes on the D4-brane do not decouple

within the supergravity approximation. For example, the mass of the lightest glueball is of the same order as the strong coupling scale. In this sense, there is no energy region, $\Lambda_{\text{QCD}} \ll E \ll M_{\text{KK}}$, in which a description in terms of weakly-coupled gluons is appropriate. Nevertheless, the qualitative features of the glueball spectrum agree with lattice calculations [3], and the supergravity description suffices, for example, to exhibit an area law for Wilson loops [2].

Since most of our phenomenological understanding of low-energy QCD comes from the study of mesons and baryons, it is interesting to construct a holographic dual of a gauge theory whose low-energy degrees of freedom consist not only of gluons but also of fundamental quarks. In the context of AdS/CFT, fundamental matter can be added to the gauge theory by introducing D-brane probes in the dual supergravity background [4, 5, 6, 7, 8, 9, 10, 11]. This has been recently exploited to study mesons holographically in several examples of gauge/gravity duals [12, 13, 14, 15]. The goal of this paper is to study a gauge/gravity dual in which the gauge theory reduces to non-supersymmetric, four-dimensional QCD in the limit in which the KK modes decouple. The construction is as follows.

Consider the D4/D6 system with the branes oriented as described by the following array:

$$\begin{array}{l} N_c \text{ D4: } 0 \ 1 \ 2 \ 3 \ 4 \ - \ - \ - \ - \ - \\ N_f \text{ D6: } 0 \ 1 \ 2 \ 3 \ - \ 5 \ 6 \ 7 \ - \ - \ . \end{array} \quad (1.1)$$

Note that the D4- and the D6-branes may be separated from each other along the 89-directions. This system is T-dual to the D3/D5 intersection, and in the decoupling limit for the D4-branes [16] provides a non-conformal version of the AdS/dCFT correspondence [5, 17]. On the gauge theory side one has a supersymmetric, five-dimensional $SU(N_c)$ gauge theory coupled to a four-dimensional defect. The entire system is invariant under eight supercharges, that is, $\mathcal{N} = 2$ supersymmetry in four-dimensional language. The degrees of freedom localized on the defect are N_f hypermultiplets in the fundamental representation of $SU(N_c)$, which arise from the open strings connecting the D4- and the D6-branes. Each hypermultiplet consists of two Weyl fermions of opposite chiralities, ψ_L and ψ_R , and two complex scalars.

As discussed above, identifying the 4-direction with period $2\pi/M_{\text{KK}}$, and with anti-periodic boundary conditions for the D4-brane fermions, breaks all of the supersymmetries and renders the theory effectively four-dimensional at energies $E \ll M_{\text{KK}}$. Further, the adjoint fermions and scalars become massive. Now, the bare mass of each hypermultiplet, m_q , is proportional to the distance between the corresponding D6-brane and the D4-branes. Even if these bare masses are zero, we expect loop effects to induce a mass for the scalars in the fundamental representation. Generation of a mass for the fundamental fermions is, however, forbidden by a chiral, $U(1)_A$ symmetry that rotates ψ_L and ψ_R with opposite phases.¹ Therefore, at low energies, we expect to be left with a four-dimensional $SU(N_c)$ gauge theory coupled to N_f flavours of fundamental quark.

In the dual string theory description, the D4-branes are again replaced by their supergravity background. In the so-called ‘probe limit’, $N_f \ll N_c$, the backreaction of the D6-branes on

¹This symmetry is broken by instanton effects, but these vanish in the large- N_c limit in which we work.

this background is negligible and hence they can be treated as probes. The D6-brane world-volume fields are dual to gauge-invariant field theory operators constructed with at least two hypermultiplet fields, that is, meson-like operators; of particular importance here will be the quark bilinear operator, $\bar{\psi}\psi \equiv \bar{\psi}_i\psi^i$, where $\psi^i = \psi_L^i + \psi_R^i$ and $i = 1, \dots, N_f$ is the flavour index. In the string description the $U(1)_A$ symmetry is nothing but the rotation symmetry in the 89-plane. In addition to acting on the fermions as explained above, this symmetry also acts on the adjoint scalar $X = X^8 + iX^9$ by a phase rotation.

Having presented the general construction, we now summarise our main results.

We begin in section 2 by considering the case of a single D6-brane. For $m_q = 0$, we expect the chiral $U(1)_A$ symmetry to be spontaneously broken by a chiral condensate, $\langle \bar{\psi}\psi \rangle \neq 0$, and there to be an associated massless, pseudo-scalar Goldstone boson in the spectrum, as in QCD with one massless flavour. In QCD, this is the η' (which becomes massless in the large- N_c limit), but, in an abuse of language, we will refer to it as a ‘pion’. We are indeed able to show that the string description provides a holographic realisation of this physics, by showing that the $U(1)_A$ symmetry is spontaneously broken by the brane embedding, as in [14]. Moreover, we numerically determine the chiral condensate for an arbitrary quark mass. We find $\langle \bar{\psi}\psi \rangle(m_q = 0) \neq 0$, as expected, and $\langle \bar{\psi}\psi \rangle(m_q) \propto 1/m_q$ for $m_q \rightarrow \infty$, again in agreement with field theory expectations (which we briefly review).

In sections 3 and 4 we study the meson spectrum. We first show analytically, in section 3, that at $m_q = 0$ there is exactly one normalisable, massless pseudo-scalar (in the four-dimensional sense) fluctuation of the D6-brane. This open-string mode corresponds precisely to the Goldstone mode of the D6-brane embedding. If $m_q > 0$, this pion becomes a pseudo-Goldstone boson. We are able to show, analytically, that its squared mass scales linearly with the quark mass, $M_\pi^2 \propto m_q$, in the limits of small (section 4) and large (section 3) quark mass. With numerical calculations we then confirm that, in fact, such a linear relation holds for all quark masses. For small m_q this linear relation is in perfect agreement with the Gell-Mann–Oakes–Renner (GMOR) relation [18],

$$M_\pi^2 = -\frac{m_q \langle \bar{\psi}\psi \rangle}{f_\pi^2}, \quad (1.2)$$

which gives the first term in the expansion of the pion mass around $m_q = 0$. In section 4, we compute the chiral condensate and the pion decay constant analytically (at $m_q = 0$), and with these results we are able to verify that, for small quark mass, the mass of our pion precisely satisfies the GMOR relation. In the opposite limit, $m_q \rightarrow \infty$, we show in section 3 that

$$M_\pi^2 = a \frac{m_q M_{\text{KK}}}{g_{\text{YM}}^2 N_c}, \quad (1.3)$$

where a is a pure number; for the lightest mesons, we find $a \sim 20$.

The remaining mesons (D6-brane excitations) are studied in section 3. For $m_q \lesssim M_{\text{susy}}$, where

$$M_{\text{susy}} = g_{\text{YM}}^2 N_c M_{\text{KK}}, \quad (1.4)$$

they all have masses of order the compactification scale, M_{KK} , and so the (pseudo-)Goldstone boson dominates the infrared physics in the regime of small m_q . Of course, this result signals the lack of decoupling between the KK and the QCD scales within the supergravity/Born–Infeld approximation, as expected. For $m_q \gtrsim M_{\text{susy}}$, supersymmetry is approximately restored, the spectrum exhibits the corresponding degeneracy, and all meson masses obey a formula like (1.3) with appropriate values of a . The fact that supersymmetry is restored at $m_q \sim M_{\text{susy}}$ suggests that the effective mass of some of the microscopic degrees of freedom must be at least of order M_{susy} . We close section 3 with an examination of certain stability issues for the D6-brane embeddings.

In section 5, for the case of multiple flavours, $N_f > 1$, we provide a holographic version of the Vafa–Witten theorem [19], which states that the $U(N_f)$ flavour symmetry cannot be spontaneously broken if $m_q > 0$. In the holographic description this is realised by the fact that the N_f D6-branes must be coincident in order to minimise their energy.

In section 6, we examine the theory at finite temperature. If $m_q > M_{\text{susy}}$, the theory exhibits two phase transitions: the first one is the well-known confinement/deconfinement transition at $T = T_{\text{deconf}} \sim M_{\text{KK}}$ [2], and the second one is a phase transition at

$$T = T_{\text{fund}} \sim \sqrt{\frac{m_q M_{\text{KK}}}{g_{\text{YM}}^2 N_c}} > T_{\text{deconf}}, \quad (1.5)$$

characterised by a discontinuity in the chiral condensate, $\langle \bar{\psi}\psi \rangle(T)$, and in the specific heat. If $m_q < M_{\text{susy}}$ the second transition does not occur as a separate phase transition.

In section 7 we discuss six-brane embeddings that, from the brane-construction viewpoint, correspond not to D4/D6 intersections but to intersections of D4-branes with D6/ $\overline{\text{D6}}$ pairs. From the gauge theory viewpoint these configurations correspond to having a defect/anti-defect pair.

We close with a brief discussion of our results in section 8. In particular, one result of the analysis of the $N_f > 1$ case in section 5 is the existence of N_f^2 massless, pseudo-scalar mesons in the gauge theory spectrum if $m_q = 0$. (We expect the inclusion of sub-leading effects in the $1/N_c$ expansion to generate small masses for these particles.) Although it is tempting to interpret these particles as Goldstone bosons of a putative, spontaneously-broken $U(N_f)_A$ chiral symmetry, we argue that this interpretation cannot be correct: even at large N_c , only one of them is a true Goldstone boson. Thus we are unable to find any obvious reasons, from the viewpoint of the four- or five-dimensional gauge theory, for these scalars to be light. We speculate that, from the string viewpoint, ten-dimensional $U(N_f)$ gauge invariance (as opposed to just seven-dimensional gauge invariance on the D6-branes) is responsible for their lightness.

2. Chiral symmetry breaking from D6-brane embeddings

In this section we will show how the spontaneous breaking of the $U(1)_A$ chiral symmetry expected from the field theory side is realized in the string description.

2.1 The D4-soliton background

The type IIA supergravity background dual to N_c D4-branes compactified on a circle with anti-periodic boundary conditions for the fermions takes the form

$$ds^2 = \left(\frac{U}{R}\right)^{3/2} (\eta_{\mu\nu} dx^\mu dx^\nu + f(U) d\tau^2) + \left(\frac{R}{U}\right)^{3/2} \frac{dU^2}{f(U)} + R^{3/2} U^{1/2} d\Omega_4^2, \quad (2.1)$$

$$e^\phi = g_s \left(\frac{U}{R}\right)^{3/4}, \quad F_4 = \frac{N_c}{V_4} \varepsilon_4, \quad f(U) = 1 - \frac{U_{\text{KK}}^3}{U^3}. \quad (2.2)$$

The coordinates $x^\mu = \{x^0, \dots, x^3\}$ parametrize the four non-compact directions along the D4-branes, as in (1.1), whereas τ parametrizes the circular 4-direction on which the branes are compactified. $d\Omega_4^2$ and ε_4 are the $SO(5)$ -invariant line element and volume form on a unit four-sphere, respectively, and $V_4 = 8\pi^2/3$ is its volume. U has dimensions of length and may be thought of as a radial coordinate in the 56789-directions transverse to the D4-branes. To avoid a conical singularity at $U = U_{\text{KK}}$, τ must be identified with period

$$\delta\tau = \frac{4\pi}{3} \frac{R^{3/2}}{U_{\text{KK}}^{1/2}}. \quad (2.3)$$

Following the nomenclature of [21], we refer to this solution as the D4-soliton.

This supergravity solution above is regular everywhere and is completely specified by the string coupling constant, g_s , the Ramond–Ramond flux quantum (*i.e.*, the number of D4-branes), N_c , and the constant U_{KK} . The remaining parameter, R , is given in terms of these quantities and the string length, ℓ_s , by

$$R^3 = \pi g_s N_c \ell_s^3. \quad (2.4)$$

If U_{KK} is set to zero, the solution (2.1, 2.2) reduces to the extremal, 1/2-supersymmetric D4-brane solution. Hence we may say that U_{KK} characterises the deviation of the D4-soliton from extremality.

The $SU(N_c)$ field theory dual to (2.1, 2.2) is defined by the compactification scale, M_{KK} , below which the theory is effectively four-dimensional, and the four-dimensional coupling constant *at* the compactification scale, g_{YM} . These are related to the string parameters by

$$M_{\text{KK}} = \frac{3 U_{\text{KK}}^{1/2}}{2 R^{3/2}} = \frac{3}{2\sqrt{\pi}} \frac{U_{\text{KK}}^{1/2}}{(g_s N_c)^{1/2} \ell_s^{3/2}}, \quad g_{\text{YM}}^2 = 3\sqrt{\pi} \left(\frac{g_s U_{\text{KK}}}{N_c \ell_s}\right)^{1/2}. \quad (2.5)$$

The first equation follows from the fact that τ is directly identified with the compact direction in the gauge theory, so $M_{\text{KK}} \equiv 2\pi/\delta\tau$. The second equation follows from the fact that $g_5^2 = (2\pi)^2 g_s \ell_s$ and the relation between the four- and five-dimensional coupling constants, $g_{\text{YM}}^2 = g_5^2/\delta\tau$, which can be seen by expanding the Born–Infeld action of the D4-brane and adopting the standard normalization for the gauge field kinetic term, $-F^2/4 g_5^2$.

It is useful to invert these relations to express the string parameters in terms of the gauge theory ones:

$$R^3 = \frac{1}{2} \frac{g_{\text{YM}}^2 N_c \ell_s^2}{M_{\text{KK}}}, \quad g_s = \frac{1}{2\pi} \frac{g_{\text{YM}}^2}{M_{\text{KK}} \ell_s}, \quad U_{\text{KK}} = \frac{2}{9} g_{\text{YM}}^2 N_c M_{\text{KK}} \ell_s^2. \quad (2.6)$$

The string length will cancel in any calculation of a physical quantity in the field theory. For example, the QCD string tension is²

$$\sigma = \frac{1}{2\pi \ell_s^2} \sqrt{-G_{tt} G_{xx}} \Big|_{U=U_{\text{KK}}} = \frac{1}{2\pi \ell_s^2} \left(\frac{U_{\text{KK}}}{R} \right)^{3/2} = \frac{2}{27\pi} g_{\text{YM}}^2 N_c M_{\text{KK}}^2. \quad (2.7)$$

Now we may ask in what situation the D4-soliton provides a reliable background in which one can study the dual field theory using only classical supergravity. First, we must require that the curvature is everywhere small compared to the fundamental string tension. This ensures that higher derivative string corrections to the low energy equations of motion are negligible. The maximum curvature in the geometry given by (2.1) occurs at precisely $U = U_{\text{KK}}$, where the curvatures are of the order $(U_{\text{KK}} R^3)^{-1/2}$. Hence we require

$$\frac{U_{\text{KK}}^{1/2} R^{3/2}}{\ell_s^2} \simeq g_{\text{YM}}^2 N_c \gg 1, \quad (2.8)$$

where we have applied the results in eq. (2.6). Therefore the restriction to small curvatures corresponds to a large 't Hooft coupling in the effective four-dimensional gauge theory, precisely as in the conventional AdS/CFT correspondence [1]. Further, to suppress string loop effects, we must also require that the local string coupling, e^ϕ , be small. Using eqs. (2.2) and (2.6) we see that, for finite values of the gauge theory parameters, the inequality $e^\phi \ll 1$ can only be satisfied up to some critical radius

$$U_{\text{crit}} \simeq \frac{N_c^{1/3} M_{\text{KK}} \ell_s^2}{g_{\text{YM}}^2}. \quad (2.9)$$

Beyond this radius, the M-theory circle opens up to reveal an $AdS_7 \times S^4$ background (with identifications). Similarly, at the corresponding high-energy scales, the five-dimensional Yang–Mills theory reveals a UV completion in terms of the (2,0) theory compactified on a circle. In the present context, we naturally demand that $U_{\text{crit}} \gg U_{\text{KK}}$, which, using (2.9) and (2.6), reduces to

$$g_{\text{YM}}^4 \ll \frac{1}{g_{\text{YM}}^2 N_c} \ll 1, \quad (2.10)$$

where the second inequality follows from eq. (2.8). Eqs. (2.8) and (2.10) imply that the supergravity analysis in the D4-soliton background is reliable in precisely the strong-coupling regime of the 't Hooft limit of the four-dimensional gauge theory: $g_{\text{YM}} \rightarrow 0$, $N_c \rightarrow \infty$, $g_{\text{YM}}^2 N_c$ fixed and large.

²This is the tension of a string lying at $U = U_{\text{KK}}$ and extending along x . It can also be computed by projecting such a string onto the boundary and integrating $\langle F^2 \rangle$ across a transverse section of the string [22].

2.2 D6-brane embeddings

We are now ready to study the embedding of a D6-brane probe in the D4-soliton geometry. Asymptotically (as $U \rightarrow \infty$), the D6-brane is embedded as described by the array (1.1). The analysis is greatly simplified by introducing isotropic coordinates in the 56789-directions. Towards this end, we first define a new radial coordinate, ρ , related to U by

$$U(\rho) = \left(\rho^{3/2} + \frac{U_{\text{KK}}^3}{4\rho^{3/2}} \right)^{2/3}, \quad (2.11)$$

and then five coordinates $\vec{z} = (z^5, \dots, z^9)$ such that $\rho = |\vec{z}|$ and $d\vec{z} \cdot d\vec{z} = d\rho^2 + \rho^2 d\Omega_4^2$. In terms of these coordinates the metric (2.1) becomes

$$ds^2 = \left(\frac{U}{R} \right)^{3/2} (\eta_{\mu\nu} dx^\mu dx^\nu + f(U) d\tau^2) + K(\rho) d\vec{z} \cdot d\vec{z}, \quad (2.12)$$

where

$$K(\rho) \equiv \frac{R^{3/2} U^{1/2}}{\rho^2}. \quad (2.13)$$

Here U is now thought of as a function of ρ . Finally, to exploit the symmetries of the D6-brane embedding we seek, we introduce spherical coordinates λ, Ω_2 for the $z^{5,6,7}$ -space and polar coordinates r, ϕ for the $z^{8,9}$ -space. The final form of the D4-brane metric is then

$$ds^2 = \left(\frac{U}{R} \right)^{3/2} (\eta_{\mu\nu} dx^\mu dx^\nu + f(U) d\tau^2) + K(\rho) (d\lambda^2 + \lambda^2 d\Omega_2^2 + dr^2 + r^2 d\phi^2), \quad (2.14)$$

where $\rho^2 = \lambda^2 + r^2$.

In these coordinates the D6-brane embedding takes a particularly simple form. We use x^μ , λ and Ω_2 (or σ^a , $a = 0, \dots, 6$, collectively) as worldvolume coordinates. The D6-brane's position in the 89-plane is specified as $r = r(\lambda)$, $\phi = \phi_0$, where ϕ_0 is a constant. Note that λ is the only variable on which r is allowed to depend, by translational and rotational symmetry in the 0123- and 567- directions, respectively. We also set $\tau = \text{constant}$ in the following, which corresponds to a single D6-brane localized in the circle direction. We will study configurations in which this condition is relaxed in section 7.

With this ansatz for the embedding, the induced metric on the D6-brane, g_{ab} , takes the form

$$ds^2(g) = \left(\frac{U}{R} \right)^{3/2} \eta_{\mu\nu} dx^\mu dx^\nu + K(\rho) [(1 + \dot{r}^2) d\lambda^2 + \lambda^2 d\Omega_2^2], \quad (2.15)$$

where $\dot{r} \equiv \partial_\lambda r$. The D6-brane action becomes

$$S_{D6} = -\frac{1}{(2\pi)^6 \ell_s^7} \int d^7\sigma e^{-\phi} \sqrt{-\det g} = -T_{D6} \int d^7\sigma \sqrt{h} \left(1 + \frac{U_{\text{KK}}^3}{4\rho^3} \right)^2 \lambda^2 \sqrt{1 + \dot{r}^2}, \quad (2.16)$$

where $T_{D6} = 2\pi/g_s(2\pi\ell_s)^7$ is the six-brane tension and h is the determinant of the metric on the round unit two-sphere. Recall that ρ is a function of λ both explicitly and through its

dependence on $r(\lambda)$. Hence the equation of motion for $r(\lambda)$ is

$$\frac{d}{d\lambda} \left[\left(1 + \frac{U_{\text{KK}}^3}{4\rho^3} \right)^2 \lambda^2 \frac{\dot{r}}{\sqrt{1+\dot{r}^2}} \right] = -\frac{3}{2} \frac{U_{\text{KK}}^3}{\rho^5} \left(1 + \frac{U_{\text{KK}}^3}{4\rho^3} \right) \lambda^2 r \sqrt{1+\dot{r}^2}. \quad (2.17)$$

Note that $r(\lambda) = r_0$, where r_0 is a constant, is a solution in the supersymmetric limit ($U_{\text{KK}} = 0$), as in [8, 12]. This reflects the BPS nature of the system, which implies that there is no force on the D6-brane regardless of its position in the 89-plane. In particular, then, the solution with $r_0 = 0$ preserves the $U(1)_A$ rotational symmetry in the 89-directions. If $U_{\text{KK}} \neq 0$ the force on the D6-brane no longer vanishes and causes it to bend as dictated by the equation of motion above. We will see below that in this case there are no (physical) solutions that preserve the $U(1)_A$ symmetry.

If $U_{\text{KK}} \neq 0$, the analysis is facilitated by rescaling to *dimensionless* variables as follows:

$$\lambda \rightarrow U_{\text{KK}} \lambda, \quad r \rightarrow U_{\text{KK}} r, \quad \rho \rightarrow U_{\text{KK}} \rho, \quad (2.18)$$

in terms of which equation (2.17) becomes

$$\frac{d}{d\lambda} \left[\left(1 + \frac{1}{4\rho^3} \right)^2 \lambda^2 \frac{\dot{r}}{\sqrt{1+\dot{r}^2}} \right] = -\frac{3}{2} \frac{1}{\rho^5} \left(1 + \frac{1}{4\rho^3} \right) \lambda^2 r \sqrt{1+\dot{r}^2}. \quad (2.19)$$

We seek solutions such that the asymptotic separation of the D6-brane and the D4-branes, L , is finite. That is, as $\lambda \rightarrow \infty$, $r(\lambda) \rightarrow r_\infty$ with

$$r_\infty = \frac{L}{U_{\text{KK}}}. \quad (2.20)$$

In the region $\lambda \rightarrow \infty$ we have $\dot{r} \rightarrow 0$ and $\rho \simeq \lambda$. Under these conditions we can linearize equation (2.19) with the result

$$\frac{d}{d\lambda} [\lambda^2 \dot{r}] \simeq -\frac{3}{2} \frac{1}{\lambda^3} r, \quad (2.21)$$

the solution to which is

$$r(\lambda) = A \frac{1}{\sqrt{\lambda}} J_{-1/3} \left(\frac{2^{1/2} 3^{-1/2}}{\lambda^{3/2}} \right) + B \frac{1}{\sqrt{\lambda}} J_{1/3} \left(\frac{2^{1/2} 3^{-1/2}}{\lambda^{3/2}} \right), \quad (2.22)$$

where J_ν are Bessel functions and A and B are arbitrary constants. For large λ , the function multiplied by A tends to a constant, whereas that multiplied by B behaves as $1/\lambda$. This means that for large λ we have

$$r(\lambda) \simeq r_\infty + \frac{c}{\lambda}, \quad (2.23)$$

where the constants r_∞ and c are related to the quark mass and the chiral condensate, as we now show.

The bare quark mass is given by the string tension times the *asymptotic* distance between the D4- and the D6-brane.³ Taking (2.20) into account, we have

$$m_q = \frac{L}{2\pi\ell_s^2} = \frac{U_{\text{KK}} r_\infty}{2\pi\ell_s^2}. \quad (2.24)$$

The quark condensate can now be computed using a simple argument. The Hamiltonian density of the theory can be written as

$$\mathcal{H} = \mathcal{H}_0 + m_q \int d^2\theta \tilde{Q}Q, \quad (2.25)$$

where \mathcal{H}_0 is m_q -independent, and \tilde{Q} , Q represent the hypermultiplet superfields in $\mathcal{N} = 1$ notation. It follows that

$$\frac{\delta\mathcal{E}}{\delta m_q} = \left\langle \int d^2\theta \tilde{Q}Q \right\rangle = \langle \bar{\psi}\psi \rangle, \quad (2.26)$$

where $\mathcal{E} = \langle \mathcal{H} \rangle$ is the vacuum energy density. In the last equality, we have assumed that the vacuum expectation value of the fundamental scalars vanishes, since they are massive (even with $m_q = 0$ after supersymmetry breaking), that is, the energy density increases if they acquire a non-zero expectation value.

Since in the string description the quark mass is given by the asymptotic position of the D6-brane, we need to evaluate the change in energy of the D6-brane associated to a change of the boundary condition r_∞ . In view of (2.16) this is given by

$$\delta\mathcal{E} = - \int d\lambda d\Omega_2 \delta\mathcal{L} = T_{\text{D6}} U_{\text{KK}}^3 \int d\lambda d\Omega_2 \delta \left[\sqrt{h} \left(1 + \frac{1}{4\rho^3} \right)^2 \lambda^2 \sqrt{1 + \dot{r}^2} \right], \quad (2.27)$$

where \mathcal{L} is the D6-brane Lagrangian density rescaled in accordance with (2.18). Using the equations of motion this becomes

$$\delta\mathcal{E} = -4\pi \left(\delta r \frac{\partial}{\partial \dot{r}} \frac{\mathcal{L}}{\sqrt{h}} \right) \Big|_{\lambda=0}^{\lambda=\infty} = 4\pi T_{\text{D6}} U_{\text{KK}}^3 \left(1 + \frac{1}{4\rho^3} \right)^2 \lambda^2 \frac{\dot{r} \delta r}{\sqrt{1 + \dot{r}^2}} \Big|_{\lambda=0}^{\lambda=\infty} = -4\pi T_{\text{D6}} U_{\text{KK}}^3 c \delta r_\infty, \quad (2.28)$$

where we used (2.23) and the fact that $\dot{r}|_{\lambda=0} = 0$, by rotational symmetry in the 567-directions. In view of (2.24) we finally obtain

$$\langle \bar{\psi}\psi \rangle = \frac{\delta\mathcal{E}}{\delta m_q} = -8\pi^2 \ell_s^2 T_{\text{D6}} U_{\text{KK}}^2 c. \quad (2.29)$$

As anticipated, the quark condensate is directly related to c ; we will see below that c is determined by r_∞ . Note that, in terms of gauge theory quantities,

$$\frac{1}{N_c} \langle \bar{\psi}\psi \rangle \simeq g_{\text{YM}}^2 N_c M_{\text{KK}}^3 c. \quad (2.30)$$

³This mass is trivially derived for the brane array (1.1) in asymptotically flat space. With supersymmetry ($U_{\text{KK}} = 0$), this bare mass persists in the decoupling limit and is then inherited by the compactified theory with supersymmetry-breaking boundary conditions, since setting $U_{\text{KK}} \neq 0$ does not alter the asymptotic properties of the model that, as usual in AdS/CFT-like dualities, determine the gauge theory parameters.

The normalization on the left-hand side is that expected in the 't Hooft limit.

We now return to the full equation of motion (2.19), which we will solve numerically. In order to understand the nature of the solutions better, however, it is helpful to first consider the limit $r_\infty \gg 1$, in which (approximate) analytical solutions can be found.

If $r_\infty \gg 1$, the entire D6-brane should lie far away from the ‘bolt’ at the center of the D4-soliton, hence we expect the solution to be a small perturbation around the solution for $U_{\text{KK}} = 0$. In other words, we set $r(\lambda) = r_\infty + \delta r(\lambda)$ and assume that $\delta r \ll 1$. Substituting this into (2.19) and expanding to linear order in δr we find

$$\frac{d}{d\lambda} (\lambda^2 \delta \dot{r}) \simeq -\frac{3}{2} \lambda^2 \frac{r_\infty}{(\lambda^2 + r_\infty^2)^{5/2}}, \quad (2.31)$$

which is easily integrated with the result

$$\delta \dot{r} \simeq -\frac{3}{2} \frac{r_\infty}{\lambda^2} \int_0^\lambda dx \frac{x^2}{(x^2 + r_\infty^2)^{5/2}} = -\frac{1}{2r_\infty} \frac{\lambda}{(\lambda^2 + r_\infty^2)^{3/2}}. \quad (2.32)$$

Here we have imposed the boundary condition $\dot{r} = 0$ at $\lambda = 0$, as required by regularity of the solution at the origin of the 567-space. Integrating once more, with the boundary condition $\delta r|_{\lambda=\infty} = 0$, we find

$$r(\lambda) \simeq r_\infty + \frac{1}{2r_\infty} \frac{1}{\sqrt{\lambda^2 + r_\infty^2}}. \quad (2.33)$$

From this large- r_∞ solution, we see that the D6-brane bends ‘outwards’, that is, it is ‘repelled’ by the D4-branes. This repulsion persists for arbitrary values of r_∞ , as is confirmed by numerical analysis. Eq. (2.19) can be integrated numerically for any value of r_∞ , and we have plotted solutions for several values of r_∞ in Figure 1.

Figure 2 displays the function $c(r_\infty)$ found by numerical integrations. As mentioned above, the value of r_∞ together with the requirement of regularity at $\lambda = 0$ (*i.e.*, $\dot{r}|_{\lambda=0} = 0$) determines the solution completely. Hence choosing r_∞ fixes $c = c(r_\infty)$. Recalling eqs. (2.24) and (2.29), which relate r_∞ and c to the quark mass and condensate, respectively, we see that this corresponds precisely to what is expected on field-theoretic grounds: once the quark mass is specified, the infrared dynamics determines the chiral condensate. In the field theory we expect the $U(1)_A$ symmetry to be spontaneously broken by a non-zero condensate in the limit $m_q \rightarrow 0$. This is indeed confirmed by the numerical results for the D6-brane embedding, since we see that, in figure 2, $c(r_\infty)$ approaches a finite constant in the limit $r_\infty \rightarrow 0$. In this limit, the asymptotic boundary condition on the D6-brane respects the rotational symmetry in the 89-plane, but it is energetically favourable for the D6-brane to bend out in the 89-plane. Hence the embedding spontaneously breaks this rotational symmetry, which matches the $U(1)_A$ symmetry-breaking in the field theory.

We see from (2.33) that $c(r_\infty) \sim 1/(2r_\infty)$ for large r_∞ , which is confirmed by the numerical results. This implies that the chiral condensate scales as $1/m_q$ for large m_q , as expected

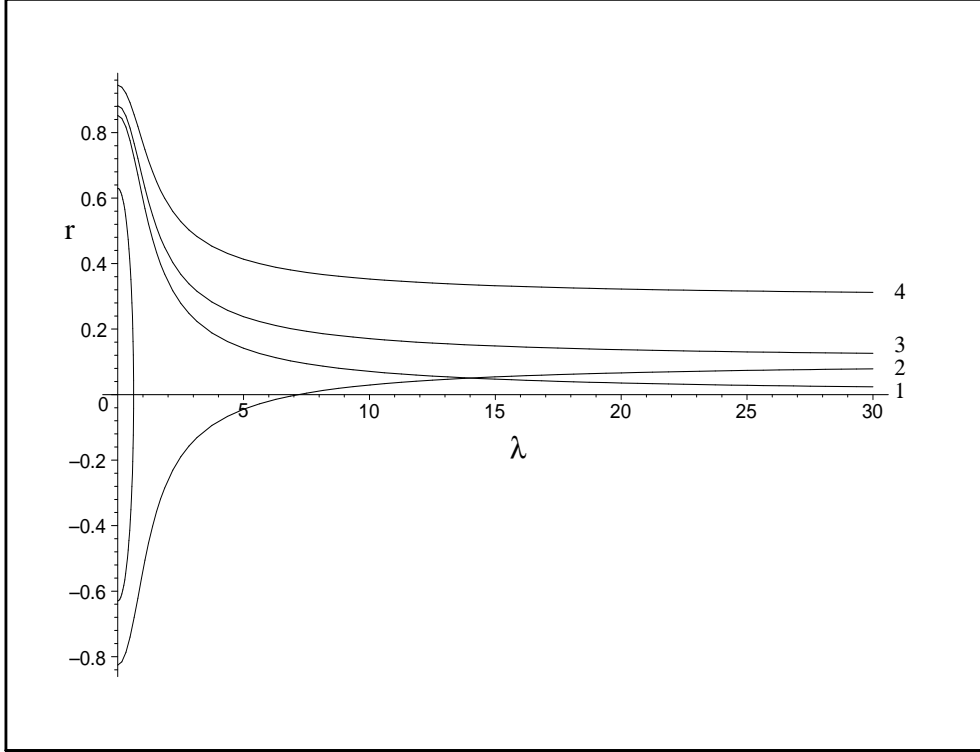


Figure 1: The D6-brane embedding for several values of the quark mass $m_q \propto r_\infty$. The interior of the ‘circle’ in the center is the region $U < U_{KK}$, which is actually not part of the space. The ‘2’ and ‘3’ embeddings correspond to the same value of r_∞ but have opposite-sign c ’s; the ‘3’ embedding has lower energy.

on field theory grounds [20]. A quick, somewhat heuristic argument for this in QCD is as follows.⁴ The trace of the energy-momentum tensor reads

$$T^\mu_{\ \mu} = m_q \bar{\psi}\psi - \frac{\alpha_s(11N_c - 2N_f)}{24\pi} \text{Tr}F^2, \quad (2.34)$$

where we have explicitly written down the classical contribution, as well as the anomalous one coming from the one-loop beta-function. In the limit $m_q \rightarrow \infty$ the theory resembles QCD with no quarks, for which

$$T^\mu_{\ \mu} = -\frac{11N_c\alpha_s}{24\pi} \text{Tr}F^2. \quad (2.35)$$

Taking vacuum expectation values and equating the two expressions we find

$$\langle \bar{\psi}\psi \rangle = \frac{\alpha_s N_f}{12\pi m_q} \langle \text{Tr}F^2 \rangle. \quad (2.36)$$

Assuming that $\langle \text{Tr}F^2 \rangle \neq 0$ we conclude that $\langle \bar{\psi}\psi \rangle \propto 1/m_q$.

⁴We thank D. T. Son for explaining this point to us.

For each value of $r_\infty > 0$, the numerical analysis actually finds two regular solutions, which have c 's of opposite sign. The curves labelled ‘2’ and ‘3’ in figure 1 are a representative example of such a pair of solutions.⁵ We have confirmed that the solutions with positive c , for which $r(\lambda) > 0$ for all λ (*e.g.*, curve 3), have the lower energy density. The negative- c solutions bend around the opposite side of the bolt at the center of the D4-soliton geometry. Naively, these solutions should be unstable, since the D6-brane is free to ‘slide off the bolt’ by moving out of the $\phi = \phi_0$ plane, and relax to the lower-energy, positive- c solution. We will return to this issue in the next section, where we study fluctuations of the D6-brane worldvolume fields around embedding solutions of each type — in fact, we will find tachyonic fluctuations for the negative- c solutions, confirming the intuition given above.

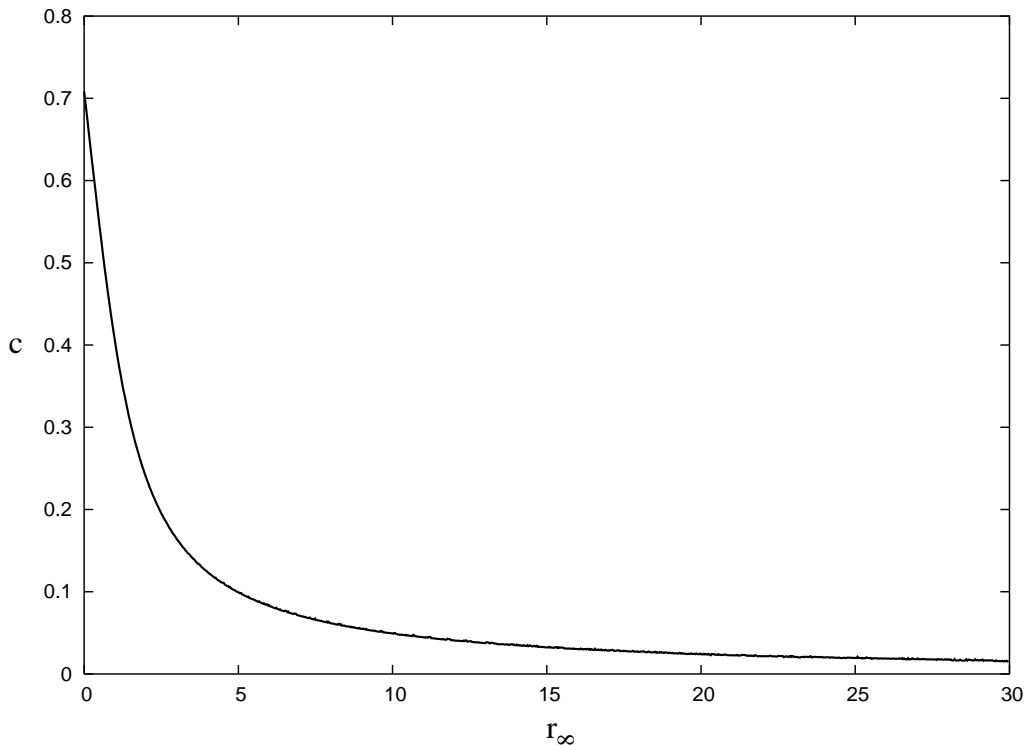


Figure 2: The quark condensate $\langle \bar{\psi}\psi \rangle \propto c$ as a function of the quark mass $m_q \propto r_\infty$.

Note that $r(\lambda) = 0$ is an exact mathematical solution of eq. (2.17) even if $U_{\text{KK}} \neq 0$. Therefore one might be tempted to conclude that it provides an alternative, $U(1)_A$ -preserving solution whose energy should be shown to be higher than that of the $U(1)_A$ -breaking solution above in order to establish spontaneous chiral symmetry breaking. However, the solution $r(\lambda) = 0$ is not physically acceptable if $U_{\text{KK}} \neq 0$ because it corresponds to an open D6-brane. That is, this solution yields a D6-brane with a boundary, which is forbidden by charge conservation. The boundary is easily seen as follows. With $r(\lambda) = 0$ we have $\rho = \lambda$, so

⁵To describe the second solution (curve 2), we allow $r(\lambda) < 0$ and restrict ϕ to the range $[0, \pi)$.

this solution terminates at the origin of the $U\tau$ -plane, that is, at $U = U_{\text{KK}}$. Since, at this point, the S^2 in the metric (2.15) still has a finite radius, $R^{3/4}U_{\text{KK}}^{1/4}$, the D6-brane would have an $\mathbb{R}^{1,3} \times S^2$ -boundary if it terminated at $U = U_{\text{KK}}$. Note that if $U_{\text{KK}} = 0$ then the two-sphere radius shrinks to zero-size and the six-brane closes off at $U = 0$. Hence the $U(1)_A$ -preserving solution $r(\lambda) = 0$ is physically sensible in the supersymmetric case. This result is in agreement with the fact that unbroken supersymmetry forbids a non-zero chiral condensate. Note, however, that this is only a formal argument, since in the limit $U_{\text{KK}} \rightarrow 0$ the curvature at $U = U_{\text{KK}}$ diverges, meaning that the supergravity description cannot be trusted in this region [16].

In section 7, we will see that the solution $r(\lambda) = 0$ can play a role in the case $U_{\text{KK}} \neq 0$ if it is simply extended past the origin of the $U\tau$ -plane. The physical interpretation of such a solution is not that of a D4/D6 intersection, but rather that of a D4/D6/ $\overline{\text{D6}}$ intersection.

3. Meson spectroscopy from D6-brane fluctuations ($N_f = 1$)

Here, we consider a certain class of fluctuations of the D6-brane around the embeddings described in the previous section. We consider first the positive- c (negative-condensate) embeddings, which were argued to be stable and so should correspond to the true ‘vacuum state’ for a given quark mass. For simplicity we restrict ourselves to fluctuations of the fields r and ϕ , as these are sufficient to illustrate the physics we wish to exhibit. We are therefore considering embeddings of the D6-brane of the form

$$\phi = 0 + \delta\phi, \quad r = r_{\text{vac}}(\lambda) + \delta r, \quad \tau = \text{constant}, \quad (3.1)$$

where the fluctuations $\delta\phi$ and δr are functions of *all* of the worldvolume coordinates and $r_{\text{vac}}(\lambda)$ is the numerically-determined vacuum embedding of the previous section.

In corroboration of our previous argument for the stability of these embeddings, we find, in particular, that the spectra of these fluctuations are non-tachyonic. We also briefly consider fluctuations around the negative- c (positive-condensate) embeddings and show their spectra do contain tachyonic modes, making manifest the instability of these configurations.

In the dual gauge theory, the r - and the ϕ -fluctuations correspond to a class of scalar and pseudo-scalar mesons, respectively. To see this, consider the complex scalar field parametrising the 89-plane, $X = X_8 + iX_9 = re^{i\phi}$. Gauge theory Lorentz transformations act only on the 0123-directions, under which X is inert, so X -fluctuations clearly correspond to spin-zero mesons. However, a parity transformation in the gauge theory corresponds to a ten-dimensional transformation that not only reverses the sign of (say) X_3 , but also replaces X by its complex conjugate, \bar{X} ; this leaves r invariant but reverses the sign of ϕ . From the gauge theory viewpoint, this is clear from the presence in the microscopic Lagrangian of a coupling of the form $\psi_R^\dagger X \psi_L + \psi_L^\dagger \bar{X} \psi_R$: the transformation $X_3 \rightarrow -X_3$ exchanges ψ_R and ψ_L , so this term is only invariant if, simultaneously, $X \rightarrow \bar{X}$. From the string theory viewpoint, the fact that only the combination of both transformations is a symmetry can be seen by examining the fermionic spectrum of the D4-D6 open strings. This arises from the zero modes of the

world-sheet fermions in the Ramond sector, that is, in the NN and DD directions: the 23- and 89-directions (in the light-cone gauge) in (1.1). Each of these modes is labelled by its weight under rotations in each of the 23- and 89-planes, (s_1, s_2) , $s_i = \pm 1/2$. The GSO projection requires $s_1 = -s_2$. Since under $X_3 \rightarrow -X_3$ we have $(s_1, s_2) \rightarrow (-s_1, s_2)$, and under $X_9 \rightarrow -X_9$ we have $(s_1, s_2) \rightarrow (s_1, -s_2)$, we see that the spectrum is only invariant under the combination of both transformations.

3.1 Analysis of the spectrum

Using the background metric (2.14) with the rescalings (2.18), the pullback of (2.14) to the embedding given in (3.1) is

$$ds^2 = \left(\frac{U}{R}\right)^{3/2} \eta_{\mu\nu} dx^\mu dx^\nu + K[(1 + r_{\text{vac}}^2)d\lambda^2 + \lambda^2 d\Omega_2^2 + 2\dot{r}_{\text{vac}} \partial_a(\delta r) d\lambda dx^a] \\ + K[\partial_a(\delta r) \partial_b(\delta r) dx^a dx^b + (r_{\text{vac}} + \delta r)^2 \partial_a(\delta\phi) \partial_b(\delta\phi) dx^a dx^b], \quad (3.2)$$

where a and b run over *all* of the worldvolume directions. To quadratic order in fluctuations, the D6-brane Lagrangian density is then

$$\mathcal{L} = \mathcal{L}_0 - T_{\text{D6}} U_{\text{KK}}^3 \lambda^2 \sqrt{h} \sqrt{1 + r_{\text{vac}}^2} \left\{ \left(\frac{3(7\rho_{\text{vac}}^2 - \lambda^2)}{16\rho_{\text{vac}}^{10}} + \frac{3(4r_{\text{vac}}^2 - \lambda^2)}{4\rho_{\text{vac}}^7} \right) (\delta r)^2 \right. \\ \left. - \frac{3r_{\text{vac}}}{4\rho_{\text{vac}}^5} \left(1 + \frac{1}{4\rho_{\text{vac}}^3} \right) \frac{\dot{r}_{\text{vac}} \partial_\lambda(\delta r^2)}{1 + r_{\text{vac}}^2} \right. \\ \left. + \left(1 + \frac{1}{4\rho_{\text{vac}}^3} \right)^2 \sum_a \frac{K}{2g_{aa}} \left(\frac{[\partial_a(\delta r)]^2}{1 + r_{\text{vac}}^2} + r_{\text{vac}}^2 [\partial_a(\delta\phi)]^2 \right) \right\}, \quad (3.3)$$

where \mathcal{L}_0 is the Lagrangian density evaluated for the vacuum embedding, as in eq. (2.16). Here, $\rho_{\text{vac}}^2 = \lambda^2 + r_{\text{vac}}^2$ and the g_{aa} in the last line correspond to the metric coefficients from eq. (2.15). In particular then, they contain no dependence on the fluctuations. Of course, integration by parts and the equation of motion (2.17) for r_{vac} allowed the terms linear in δr to be eliminated.

The linearised equations of motion that follow are, for $\delta\phi$:

$$\frac{9}{4M_{\text{KK}}^2} \frac{r_{\text{vac}}^2}{\rho_{\text{vac}}^3} \left(1 + \frac{1}{4\rho_{\text{vac}}^3} \right)^{4/3} \partial_\mu \partial^\mu(\delta\phi) + \frac{r_{\text{vac}}^2}{\lambda^2} \left(1 + \frac{1}{4\rho_{\text{vac}}^3} \right)^2 \nabla^2(\delta\phi) \\ + \frac{1}{\lambda^2 \sqrt{1 + r_{\text{vac}}^2}} \frac{d}{d\lambda} \left[\frac{\lambda^2 r_{\text{vac}}^2}{\sqrt{1 + r_{\text{vac}}^2}} \left(1 + \frac{1}{4\rho_{\text{vac}}^3} \right)^2 \partial_\lambda(\delta\phi) \right] = 0, \quad (3.4)$$

and, for δr :

$$\frac{\lambda^2}{\sqrt{1 + r_{\text{vac}}^2}} \left[\frac{9}{4M_{\text{KK}}^2} \frac{1}{\rho_{\text{vac}}^3} \left(1 + \frac{1}{4\rho_{\text{vac}}^3} \right)^{4/3} \partial_\mu \partial^\mu(\delta r) + \frac{1}{\lambda^2} \left(1 + \frac{1}{4\rho_{\text{vac}}^3} \right)^2 \nabla^2(\delta r) \right]$$

$$\begin{aligned}
& + \frac{d}{d\lambda} \left[\frac{\lambda^2}{(1+r_{\text{vac}}^2)^{3/2}} \left(1 + \frac{1}{4\rho_{\text{vac}}^3}\right)^2 \partial_\lambda(\delta r) \right] - \frac{d}{d\lambda} \left[\frac{3\lambda^2 r_{\text{vac}} \dot{r}_{\text{vac}}}{2\rho_{\text{vac}}^5 \sqrt{1+r_{\text{vac}}^2}} \left(1 + \frac{1}{4\rho_{\text{vac}}^3}\right) \right] \delta r \\
& - \lambda^2 \sqrt{1+r_{\text{vac}}^2} \left(\frac{3(7r_{\text{vac}}^2 - \lambda^2)}{8\rho_{\text{vac}}^{10}} + \frac{3(4r_{\text{vac}}^2 - \lambda^2)}{2\rho_{\text{vac}}^7} \right) \delta r = 0. \quad (3.5)
\end{aligned}$$

In these expressions, ∇^2 is the Laplacian on the two-sphere.

From the form of the equations of motion, it is clear that we may separate variables to write

$$\delta\phi = \mathcal{P}(\lambda) e^{ik_\phi \cdot x} Y_{\ell_\phi m_\phi}(S^2), \quad \delta r = \mathcal{R}(\lambda) e^{ik_r \cdot x} Y_{\ell_r m_r}(S^2), \quad (3.6)$$

where $Y_{\ell m}$ are the conventional spherical harmonics. We then look for normalizable solutions with definite S^2 -angular momentum $\ell_{\phi,r}$ and four-dimensional mass $M_{\phi,r}^2 = -k_{\phi,r}^2$. For the sake of simplicity in the following, we only focus on the case $\ell_{\phi,r} = 0$ and find the lowest-mass modes for each fluctuation.

We employ the shooting method to solve the linearized equations of motion. First we use the asymptotic form of the equations for $\lambda \rightarrow \infty$ and the requirement of normalizability to determine the asymptotic boundary conditions for the fluctuations. Then we vary the four-dimensional mass parameters until, by numerically integrating the equation of motion, we find solutions that are also regular at the origin. Recall⁶ that the asymptotic behaviour of the vacuum profile is $r_{\text{vac}} \simeq r_\infty + c/\lambda$, where r_∞ is related to the quark mass by equation (2.24). In this asymptotic region we have that $\rho_{\text{vac}}(\lambda) \simeq \lambda$, so the equation of motion for $\delta\phi$ becomes, approximately,

$$\frac{9M_\phi^2}{4M_{\text{KK}}^2} \frac{r_{\text{vac}}^2}{\lambda} (\delta\phi) + \frac{d}{d\lambda} [\lambda^2 r_{\text{vac}}^2 \partial_\lambda (\delta\phi)] = 0, \quad (3.7)$$

and similarly that for δr becomes

$$\frac{9M_r^2}{4M_{\text{KK}}^2} \frac{1}{\lambda} (\delta r) + \frac{d}{d\lambda} [\lambda^2 \partial_\lambda (\delta r)] = 0. \quad (3.8)$$

It follows that the asymptotic behaviour of $\delta r(\lambda)$ does not depend on that of $r_{\text{vac}}(\lambda)$, whereas that of $\delta\phi(\lambda)$ depends crucially on whether or not $r_\infty = 0$, that is, whether or not the quarks are massless. We will now show that if $r_\infty = 0$ then there exists a normalizable $\delta\phi$ mode with $M_\phi = 0$, whereas if $r_\infty \neq 0$ there is a mass gap in the spectrum.

If we set $r_\infty = 0$, we find that the asymptotic equation for $\delta\phi$ becomes

$$\frac{9M_\phi^2}{4M_{\text{KK}}^2} \frac{1}{\lambda^3} (\delta\phi) + \partial_\lambda^2 (\delta\phi) = 0. \quad (3.9)$$

The first term is sub-leading for large λ , so we may drop it to find that the asymptotic form of $\delta\phi$, regardless of the value of M_ϕ , is

$$\delta\phi \simeq b + a\lambda, \quad (3.10)$$

⁶Also recall that we are working with dimensionless variables r and λ , rescaled as in eq. (2.18).

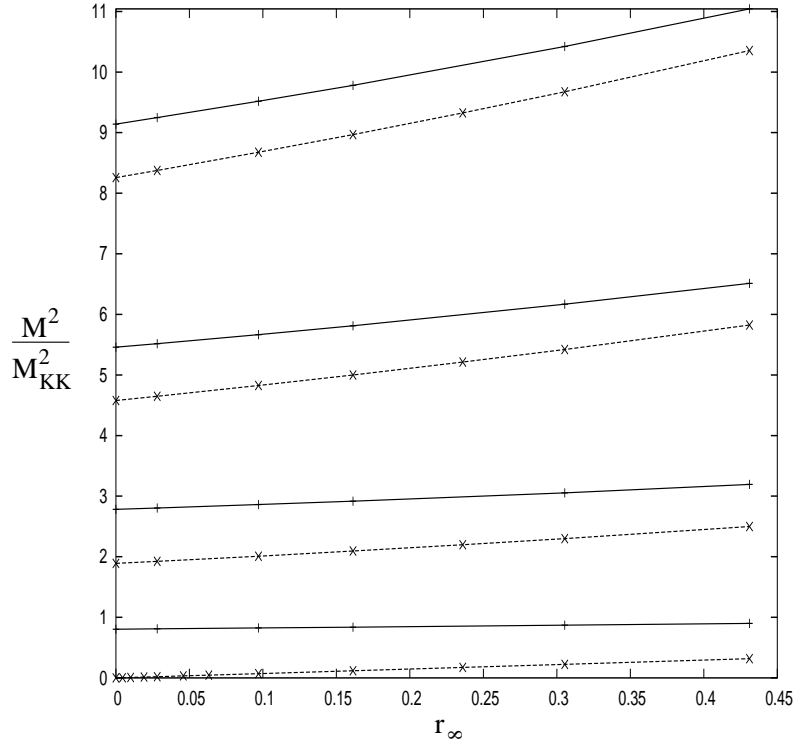


Figure 3: Squared masses for the four lowest-lying $\delta\phi$ modes (dashed lines), dual to pseudo-scalar mesons, and the four lowest-lying δr modes (solid lines), dual to scalar mesons, as functions of the quark mass $m_q \propto r_\infty$.

where a and b are arbitrary constants. For $r_\infty \neq 0$, however, we find that

$$\frac{9M_\phi^2}{4M_{\text{KK}}^2} \frac{1}{\lambda^3} (\delta\phi) + \frac{2}{\lambda} \partial_\lambda (\delta\phi) + \partial_\lambda^2 (\delta\phi) = 0. \quad (3.11)$$

Again the first term is sub-leading for large λ , so the solution is

$$\delta\phi \simeq \tilde{a} + \tilde{b}/\lambda. \quad (3.12)$$

Normalizable solutions correspond to the boundary conditions $a = 0$ and $\tilde{a} = 0$ in the cases $r_\infty = 0$ and $r_\infty \neq 0$, respectively, since the terms with coefficients b and \tilde{b} are the ones that fall off more rapidly at infinity. Since the differential equations we are solving are linear, we may choose $b = \tilde{b} = 1$ without loss of generality, so we are left with the boundary conditions $\{\delta\phi = 1, \delta\phi' = 0\}|_{\lambda \rightarrow \infty}$ if $r_\infty = 0$, and $\{\delta\phi = 1/\lambda, \delta\phi' = -1/\lambda^2\}|_{\lambda \rightarrow \infty}$ if $r_\infty \neq 0$. A similar analysis for the δr fluctuations shows that they obey the same asymptotic equation of motion as the $\delta\phi$ fluctuations in the $r_\infty \neq 0$ case, so the appropriate boundary conditions are $\{\delta r = 1/\lambda, \delta r' = -1/\lambda^2\}|_{\lambda \rightarrow \infty}$.

Now note that $\delta\phi = e^{ik_\phi \cdot x}$, with $k_\phi^2 = 0$, is an exact, regular solution of (3.4) with zero four-dimensional mass (and $\nabla^2(\delta\phi) = 0$), which is normalisable *only* if $r_\infty = 0$. This means

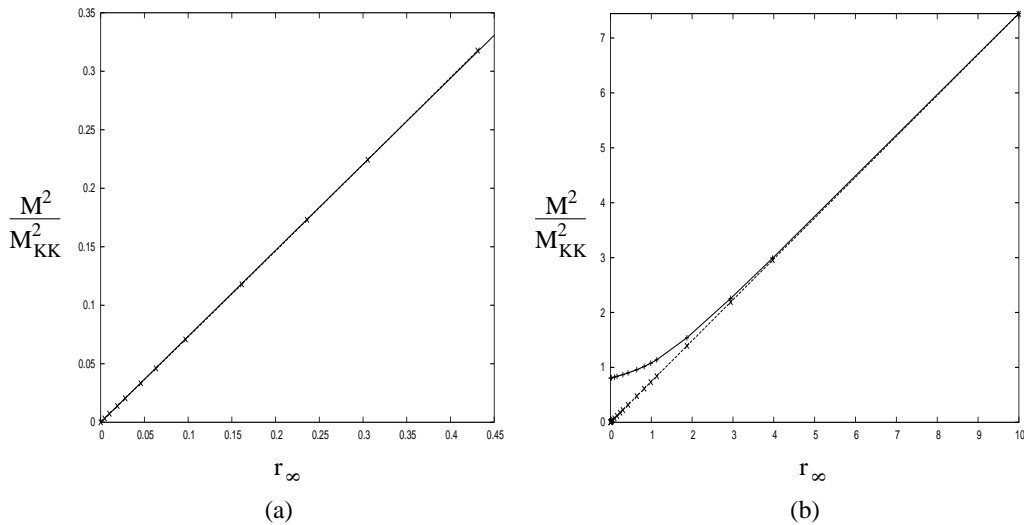


Figure 4: (a) Linear fit of the lowest-lying $\delta\phi$ mode for different values of $m_q \sim r_\infty$. (b) Degeneracy of the lowest-lying $\delta\phi$ (dashed) and δr (solid) modes in the supersymmetric limit $r_\infty \gg 1$.

that with massless quarks there is a massless, pseudo-scalar meson in the spectrum of the gauge theory, whose dual is the zero-mode fluctuation of the D6-brane field ϕ . The mathematical form of these fluctuations shows that they correspond to rotations of the vacuum embedding in the 89-plane. Of course, this form is precisely as expected for the Goldstone mode associated with the spontaneous breaking of this rotational symmetry.

The shooting technique allows us to verify this numerically, and to find the values of $M_{\phi,r}$ for which other normalizable, regular solutions exist. The results are the low-lying (pseudo)scalar meson spectra, which are displayed in Figure 3 for different values of the quark mass. As anticipated, there is no mass gap in the ϕ -meson spectrum when the quark is massless. There is a smooth transition to a theory with a mass gap as the quark mass is increased and, in fact, a best-fit (shown in figure 4a) yields a linear relationship,⁷ $M_\phi^2 \simeq 0.73 M_{\text{KK}}^2 r_\infty$, for small $r_\infty \propto m_q$, as expected from the GMOR relationship (1.2), which we will reproduce analytically in the next section.

As shown in figure 3, there are no normalisable, regular solutions of equation (3.5) with $M_r = 0$, so there is a mass gap in the r -meson spectrum regardless of the value of the quark mass. For small quark mass the mass scale of all of the mesons, except the lowest-lying $\delta\phi$ mode, is⁸

$$M^2 \sim M_{\text{KK}}^2 \sim \frac{U_{\text{KK}}}{R^3}. \quad (3.13)$$

This is another reflection of the lack of decoupling between the QCD scale and the compactification scale.

⁷An analogous relationship was observed in [14].

⁸This also sets the scale of the glueball mass spectrum [3].

As suggested by Figure 3, the r - and ϕ -mesons occur in pairs that become degenerate for large enough a quark mass. The reason is that, in the supersymmetric case ($U_{\text{KK}} = 0$), these mesons belong to the same supermultiplet and hence have equal masses, as in [12]. If $U_{\text{KK}} \neq 0$ this degeneracy is only approximate for quark masses much larger than the supersymmetry-breaking scale, M_{susy} , becoming exact in the limit $m_q \rightarrow \infty$. Geometrically, this corresponds to the fact that the distortion of the D6-brane away from the flat, supersymmetric profile decreases the farther away from the D4-branes we embed it. Since this distance scale is measured by $L \propto m_q$, and U_{KK} characterises the supersymmetry breaking, we expect that, for $L \gg U_{\text{KK}}$, the characteristic mass scale of the mesons should become independent of U_{KK} and depend, instead, on some ratio of L and R . To see that this is indeed the case, we approximate the vacuum profile by the flat solution in equations (3.4) and (3.5), that is, we set $r_{\text{vac}}(\lambda) = r_\infty$, and we expand these equations assuming that $r_\infty \gg 1$. In terms of a new variable $y = \lambda/L$ we obtain (for zero S^2 -angular momentum)

$$\frac{R^3 M_\phi^2}{L(y^2 + 1)^{3/2}} \delta\phi + \frac{1}{y^2} \frac{d}{dy} [y^2 \partial_y \delta\phi] = 0, \quad (3.14)$$

and

$$\frac{R^3 M_r^2}{L(y^2 + 1)^{3/2}} \delta r + \frac{1}{y^2} \frac{d}{dy} [y^2 \partial_y \delta r] = 0. \quad (3.15)$$

The fact that the two types of fluctuations satisfy the same equation confirms that the spectrum becomes degenerate in this limit. It is also clear that the mass scale for the mesons in this limit is now

$$M^2 \sim \frac{L}{R^3} \sim \frac{m_q M_{\text{KK}}}{g_{\text{YM}}^2 N_c}, \quad (3.16)$$

since this is the only scale that appears in eq. (3.14), (3.15).

The transition between the regimes (3.13) and (3.16) occurs at $L \sim U_{\text{KK}}$, and is illustrated for the lightest r - and ϕ -mesons in figure 4b, which was generated by solving equations (3.4) and (3.5) numerically. The figure clearly illustrates the degeneracy of the modes in the expected regime. The condition $L \sim U_{\text{KK}}$ translates into $m_q \sim M_{\text{susy}}$, with M_{susy} as defined in (1.4), so M_{susy} is indeed the scale at which supersymmetry is restored, as suggested by our choice of notation. Note that at the transition point, at which of course eqs. (3.13) and (3.16) coincide, we have $M \sim m_q / (g_{\text{YM}}^2 N_c)$. As we are working in the 't Hooft limit of the gauge theory, these mesons are very deeply bound, *i.e.*, $M \ll 2m_q$. The suppression of these meson masses by the 't Hooft coupling is even stronger than that found in a similar context in [12], where $M \sim m_q / \sqrt{g_{\text{YM}}^2 N_c}$. For large quark mass there is an extra suppression implicit in eq. (3.16) due to the fact that M^2 scales linearly in m_q , as opposed to quadratically.

As we are working in a range where we expect the gauge theory is five-dimensional, it is perhaps more appropriate to re-express the transition scale in terms of the five-dimensional gauge coupling; it then reads $m_q \sim g_5^2 N_c M_{\text{KK}}^2$. Similarly, the mass scale typical of the mesons becomes $M^2 \sim m_q / (g_5^2 N_c)$. In any event, the transition scale suggests that the effective mass squared of some of the microscopic degrees of freedom must be at least of the order

$M_{\text{susy}} \gg M_{\text{KK}}$, rather than just M_{KK} . Note that this mass scale is a factor of $\sqrt{g_{\text{YM}}^2 N_c}$ larger than that coming from a simple one-loop calculation for the scalar masses, which yields $\sqrt{g_{\text{YM}}^2 N_c} M_{\text{KK}}$. This factor seems to be ubiquitous in extrapolations from weak to strong 't Hooft coupling in the context of AdS/CFT.

As we saw above, the squared masses of all mesons scale linearly in the quark mass as $m_q \rightarrow \infty$. For the lightest meson, the results displayed in figure 4b seem to indicate that, in fact, this linear relationship is valid not only in the limits of small and large m_q , but for all quark masses. This result has been confirmed to within the best accuracy of our numerical analysis. Unfortunately, eq. (3.14) has four regular singular points and so no closed-form analytic solution is available, but its numerical solution gives, for the lowest-mass modes,

$$M^2 \simeq 1.66 \frac{L}{R^3} \simeq 20.91 \frac{M_{\text{KK}}}{g_{\text{YM}}^2 N_c} m_q \simeq 0.74 M_{\text{KK}}^2 r_\infty . \quad (3.17)$$

The final form of this expression agrees with a best-fit of the data plotted in the region of figure 4b with $r_\infty \gg 1$ and, in principle, describes the extension of this figure to arbitrarily high values of r_∞ . We therefore conclude that, in our model, the GMOR linear relation between M_π^2 and m_q extrapolates to all quark masses.

3.2 Stability Issues

Recall that, at the end of section 2, we remarked that our numerical integrations had revealed two classes of six-brane embeddings, those with positive c and those with negative c . From the numerical analysis, we could show that, for a given r_∞ , the positive- c or negative-condensate solutions had the lower energy density. Further we argued that the negative- c solutions should be unstable.

The stability of the negative-condensate (positive- c) vacuum embedding is reflected in the fact that the spectrum of fluctuations does not contain tachyonic modes. While numerical searches did not reveal any tachyonic fluctuations, one can formulate a general argument that no such modes can exist in the spectrum of $\delta\phi$.⁹ Consider the equation of motion (3.4) (with zero angular momentum on the two-sphere, for simplicity). Multiplying by $\delta\phi$, integrating over λ and integrating by parts, yields

$$\begin{aligned} \int_0^\infty d\lambda \left\{ \frac{9M_\phi^2}{4M_{\text{KK}}^2} \frac{\lambda^2 r_{\text{vac}}^2}{\rho_{\text{vac}}^3} \left(1 + \frac{1}{4\rho_{\text{vac}}^3}\right)^{4/3} \sqrt{1 + \dot{r}_{\text{vac}}^2} \delta\phi^2 - \frac{\lambda^2 r_{\text{vac}}^2}{\sqrt{1 + \dot{r}_{\text{vac}}^2}} \left(1 + \frac{1}{4\rho_{\text{vac}}^3}\right)^2 [\partial_\lambda(\delta\phi)]^2 \right\} \\ = \left[\frac{\lambda^2 r_{\text{vac}}^2}{\sqrt{1 + \dot{r}_{\text{vac}}^2}} \left(1 + \frac{1}{4\rho_{\text{vac}}^3}\right)^2 \delta\phi \partial_\lambda(\delta\phi) \right]_0^\infty = 0 . \end{aligned} \quad (3.18)$$

Note that we were able to set the term on the right-hand side to zero using the behaviour of the normalizable $\delta\phi$ modes at $\lambda = 0$ and $\lambda = \infty$. On the left-hand side, the second term in

⁹We expect that these arguments extend to δr fluctuations but we did not explicitly consider these modes a possible decay channel between the two D6-brane embeddings, due to the geometric obstruction provided by the 'bolt' at the centre of the D4-soliton.

the integrand is manifestly negative or zero, while the sign of the first term depends on that of M_ϕ^2 . Therefore, for tachyonic modes it is clear that the integral will be negative-definite, which is inconsistent with the vanishing of the right-hand side. The argument extends to include nonvanishing ℓ_ϕ , which simply introduces an additional negative-definite term under the integral. Hence we conclude that the negative-condensate embeddings are free from tachyonic instabilities in this sector. As this was the sector with the lowest lying mode, we might have expected it to be the most potentially problematic with regards to stability. Hence we are confident that these positive- c solutions are stable.

Now we turn our attention to the negative- c or positive-condensate embeddings. Recall that our intuition was that these solutions should be unstable to ‘sliding off the bolt.’ Since the embedding coordinate (r , here) always vanishes at some value of λ for this case, we cannot address the issue of such an instability using the $\delta\phi$ equation of motion, since ϕ is not everywhere well-defined. Hence, we change to Cartesian coordinates X and Y in the $r\phi$ -plane. With the choice that the D6-brane lies at $\phi_{\text{vac}}(\lambda) = \phi_0 = 0$ (*i.e.*, $Y_{\text{vac}}(\lambda) = 0$), it follows that the embedding profile in X satisfies the equation of motion (2.19) and we may set $X_{\text{vac}}(\lambda) = r_{\text{vac}}(\lambda)$. Fluctuations in $Y(\lambda)$ are now the modes relevant for stability and have the benefit of being well-defined for all λ . One finds the following equation of motion for these fluctuations:

$$\begin{aligned} & \frac{9}{4M_{\text{KK}}^2} \frac{1}{\rho_{\text{vac}}^3} \left(1 + \frac{1}{4\rho_{\text{vac}}^3}\right)^{4/3} \partial_\mu \partial^\mu (\delta Y) + \frac{1}{\lambda^2} \left(1 + \frac{1}{4\rho_{\text{vac}}^3}\right)^2 \nabla^2 (\delta Y) \\ & + \frac{1}{\lambda^2 \sqrt{1 + \dot{X}_{\text{vac}}^2}} \frac{d}{d\lambda} \left[\frac{\lambda^2}{\sqrt{1 + \dot{X}_{\text{vac}}^2}} \left(1 + \frac{1}{4\rho_{\text{vac}}^2}\right)^2 \partial_\lambda (\delta Y) \right] + \frac{3(1 + 4\rho_{\text{vac}}^3)}{8\rho_{\text{vac}}^8} \delta Y = 0, \end{aligned} \quad (3.19)$$

where, now, $\rho_{\text{vac}}^2 = \lambda^2 + X_{\text{vac}}^2$. Making a stability argument along the lines of that given above for $\delta\phi$ is no longer possible, due to the presence of the final term in (3.19). This term introduces into the integrand analogous to that in eq. (3.18) a contribution that is manifestly positive. Hence this approach does not yield a definite conclusion in this case.

However, it is still possible to look directly for tachyonic modes in the spectrum of fluctuations around the negative- c embeddings using our numerical techniques. From eq. (3.19) one can deduce the asymptotic behaviour of the δY modes to be

$$\delta Y \simeq \tilde{a} + \tilde{b}/\lambda, \quad (3.20)$$

independent of the vacuum embedding. Using the shooting method as before, the spectrum of each positive-condensate embedding considered numerically is found to contain a tachyonic mode and, furthermore, these modes become ‘more tachyonic’ as the quark mass increases — see figure 5. As is suggested in the figure, the squared mass of the lowest-lying δY mode has a linear dependence on the quark mass. In fact, a best-fit of the data gives $M_Y^2 \simeq -0.72 M_{\text{KK}}^2 r_\infty$.

An examination of the next-to-lowest-lying δY mode (not shown in the figure) indicates that the mass of this mode, which is real and positive for $m_q = 0$, also decreases as a function

of r_∞ . So for sufficiently large quark mass the spectrum may contain more than one tachyon. However, we could not confirm this directly because for large r_∞ the negative- c embeddings approach extremely close to the bolt, and our computer code behaved erratically in this situation.

4. The pseudo-Goldstone boson

As discussed in the previous section, if $m_q = 0$ the spectrum contains a massless, pseudo-scalar mode that can be understood as the Goldstone boson of the spontaneously broken $U(1)_A$ symmetry. This is akin to the η' meson in QCD, which is massless in the large- N_c limit. In an abuse of language, however, we will refer to this Goldstone boson as a ‘pion’. For non-zero quark mass, the $U(1)_A$ symmetry is explicitly broken and the pion becomes a pseudo-Goldstone boson with a mass M_π that, according to our numerical analysis, grows as $M_\pi^2 \sim m_q$. This means that at low energies, $E \ll \Lambda_{\text{QCD}}$, the dynamics is dominated by this particle. In this section we will provide an analytic proof, using the string description, that the pion’s mass actually obeys the well-known Gell-Mann–Oakes–Renner relation (1.2).

Recall that the gauge theory pion is dual to a ϕ -fluctuation of the D6-brane of the form $\delta\phi = e^{ik \cdot x} \varphi(\lambda)$ that solves equation (3.4) with $\nabla^2(\delta\phi) = 0$, that is,

$$\frac{d}{d\lambda} [p(\lambda)\dot{\varphi}] = -M^2\mu(\lambda)\varphi, \quad (4.1)$$

where $M^2 = -k^2$ is the four-dimensional mass,

$$p(\lambda) = \lambda^2 r_{\text{vac}}^2 \left(1 + \frac{1}{4\rho_{\text{vac}}^3}\right)^2 \frac{1}{\sqrt{1 + \dot{r}_{\text{vac}}^2}}, \quad (4.2)$$

$$\mu(\lambda) = \lambda^2 \frac{9}{4M_{\text{KK}}^2} \frac{r_{\text{vac}}^2}{\rho_{\text{vac}}^3} \left(1 + \frac{1}{4\rho_{\text{vac}}^3}\right)^{4/3} \sqrt{1 + \dot{r}_{\text{vac}}^2}, \quad (4.3)$$

and $\rho_{\text{vac}}^2 = \lambda^2 + r_{\text{vac}}^2$. The allowed solutions are those that both satisfy $\dot{\varphi}|_{\lambda=0} = 0$ and are normalizable with respect to the scalar product

$$\langle \varphi_1 | \varphi_2 \rangle = \int_0^\infty d\lambda \mu(\lambda) \varphi_1^*(\lambda) \varphi_2(\lambda). \quad (4.4)$$

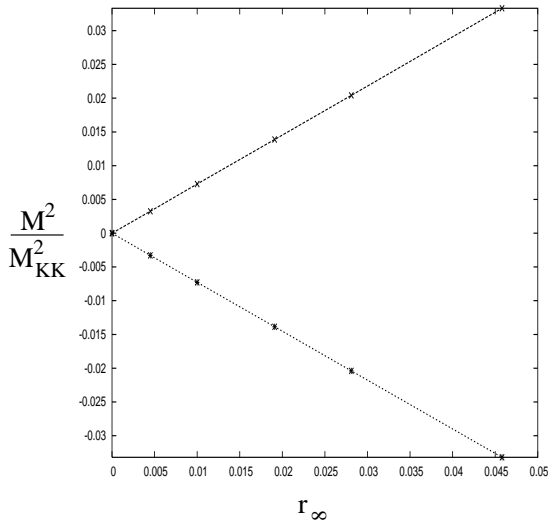


Figure 5: The lowest-lying δY mode for some negative-condensate embeddings (upper line), and the lowest-lying δY mode for the corresponding positive-condensate embeddings (lower line) — the δY modes are tachyonic.

This defines an eigenvalue problem whose solution is a complete set of orthogonal eigenfunctions φ_n with eigenvalues M_n^2 . Notice that if $\varphi(\lambda) = \text{constant}$ then the eigenvalue equation is satisfied with $M^2 = 0$, but the mode is normalizable only if $r_{\text{vac}}(\lambda) \rightarrow 0$ as $\lambda \rightarrow \infty$. If $\varphi(\lambda)$ is not constant, multiplying eq.(4.1) by φ , integrating both sides with respect to λ and performing an integral by parts in the left-hand side, we arrive at

$$M^2 = \frac{\int_0^\infty d\lambda p(\lambda) \dot{\varphi}^2}{\int_0^\infty d\lambda \mu(\lambda) \varphi^2} > 0 . \quad (4.5)$$

Since from (4.2) and (4.3) we have $p(\lambda) > 0$ and $\mu(\lambda) > 0$, it follows that M^2 is positive, as indicated.¹⁰

Having said that, we now want to compute the mode with lowest eigenvalue $M^2 > 0$ when m_q is non-vanishing but small, that is, let us suppose that $r_{\text{vac}} \rightarrow r_\infty$ as $\lambda \rightarrow \infty$, with r_∞ small but non-zero. In this case we expect that the normalizable eigenmode can be obtained from the massless-quark zero-mode, namely $\varphi(\lambda) = \text{constant}$, by using perturbation theory. To this end, it is convenient to define

$$\psi(\lambda) = \sqrt{p(\lambda)} \varphi(\lambda) , \quad (4.6)$$

which satisfies the new eigenvalue equation

$$\ddot{\psi} - \frac{\ddot{\Psi}}{\Psi} \psi = -M^2 \nu \psi , \quad (4.7)$$

where $\Psi = \sqrt{p}$, and $\nu = \mu/p$ is the new integration measure. If $r_\infty = 0$ then $\psi(\lambda) = \Psi(\lambda)$ is a normalizable solution of (4.7) with zero eigenvalue. Making a small change in the boundary condition, $r_\infty \rightarrow \delta r_\infty \gtrsim 0$, induces a small change in the vacuum profile $r_{\text{vac}}(\lambda)$, which in turn induces a small change in the functions $\Psi(\lambda)$ and $\nu(\lambda)$ appearing in equation (4.7). Standard quantum mechanics perturbation theory can then be applied to obtain the new lowest eigenvalue.

Let us denote with a ‘bar’ the quantities corresponding to $r_\infty = 0$, so that for $r_\infty \neq 0$ we have

$$\Psi = \bar{\Psi} + \delta\Psi , \quad (4.8)$$

$$\nu = \bar{\nu} + \delta\nu , \quad (4.9)$$

where $\delta\Psi$ and $\delta\nu$ are the differences induced by the change in $r_{\text{vac}}(\lambda)$. The new lowest eigenvalue and its associated wave-function, $M^2 \gtrsim 0$ and $\psi = \bar{\Psi} + \delta\psi$, obey, to leading order,

$$\delta\ddot{\psi} - \frac{\ddot{\Psi}}{\Psi} \delta\psi - \delta \left(\frac{\ddot{\Psi}}{\Psi} \right) \bar{\Psi} = -M^2 \bar{\nu} \bar{\Psi} . \quad (4.10)$$

¹⁰This is not valid when r_{vac} vanishes at some point (which is not the case studied here) — see the more detailed discussion after equation (3.18).

Decomposing $\delta\psi$ as a linear combination of massless-quark eigenfunctions, $\delta\psi = \sum_{n=0}^{\infty} \alpha_n \bar{\psi}_n$, we obtain

$$\sum_{n=1}^{\infty} \alpha_n \bar{M}_n^2 \bar{\nu} \bar{\psi}_n + \delta \left(\frac{\ddot{\Psi}}{\Psi} \right) \bar{\Psi} = M^2 \bar{\nu} \bar{\Psi}, \quad (4.11)$$

where we have dropped the first term in the series, using $\bar{M}_0 = 0$. Multiplying by $\bar{\Psi}$, integrating over λ and using the orthogonality condition $\int_0^{\infty} d\lambda \bar{\nu} \bar{\Psi} \bar{\psi}_n = 0$ for $n > 0$ (since $\bar{\Psi}$ is the zero-mode eigenfunction and is real) we deduce that

$$M^2 \int_0^{\infty} d\lambda \bar{\nu} \bar{\Psi}^2 = \int_0^{\infty} d\lambda \delta \left(\frac{\ddot{\Psi}}{\Psi} \right) \bar{\Psi}^2 = \int_0^{\infty} d\lambda (\bar{\Psi} \delta \ddot{\Psi} - \ddot{\Psi} \delta \bar{\Psi}) = \left[\bar{\Psi} \delta \dot{\Psi} - \dot{\Psi} \delta \bar{\Psi} \right]_{\lambda=0}^{\lambda=\infty}. \quad (4.12)$$

Recalling that

$$\bar{\Psi} = \lambda \bar{r}_{\text{vac}} \left(1 + \frac{1}{4\bar{\rho}_{\text{vac}}^3} \right) (1 + \dot{r}_{\text{vac}}^2)^{-1/4}, \quad (4.13)$$

which implies

$$\begin{aligned} \delta \bar{\Psi} = & \lambda \delta r_{\text{vac}} \left(1 + \frac{1}{4\bar{\rho}_{\text{vac}}^3} \right) (1 + \dot{r}_{\text{vac}}^2)^{-1/4} - \frac{3\lambda \dot{r}_{\text{vac}}^2}{4\bar{\rho}_{\text{vac}}^5} (1 + \dot{r}_{\text{vac}}^2)^{-1/4} \delta r_{\text{vac}} - \\ & - \lambda \bar{r}_{\text{vac}} \left(1 + \frac{1}{4\bar{\rho}_{\text{vac}}^3} \right) \frac{1}{2} (1 + \dot{r}_{\text{vac}}^2)^{-5/4} \dot{r}_{\text{vac}} \delta \dot{r}_{\text{vac}}, \end{aligned} \quad (4.14)$$

we see that the only contribution to the last term in equation (4.12) comes from $\lambda = \infty$. This is easily evaluated, since for large λ we have

$$\bar{r}_{\text{vac}} \simeq \frac{\bar{c}}{\lambda} + \mathcal{O}\left(\frac{1}{\lambda^2}\right), \quad \bar{\Psi} \simeq \lambda \bar{r}_{\text{vac}} \simeq \bar{c} + \mathcal{O}\left(\frac{1}{\lambda}\right). \quad (4.15)$$

It follows that the new eigenvalue is given by

$$M^2 = \frac{\bar{c} \delta r_{\infty}}{\int_0^{\infty} d\lambda \bar{\nu} \bar{\Psi}^2} = \frac{\bar{c} \delta r_{\infty}}{\int_0^{\infty} d\lambda \bar{\mu}}. \quad (4.16)$$

To show that this formula is precisely the GMOR relation (1.2), we need to identify the pion decay constant in the string description. In this description, a shift of the chiral angle that parametrizes the space of vacua related to each other by the $U(1)_A$ symmetry corresponds to a rigid rotation of the D6-brane field ϕ (both take values between 0 and 2π). Similarly, the pion field is identified with the normalizable, massless mode $\delta\phi$, described in section 3.1. The pion decay constant can be read off from the normalization of the kinetic term in the four-dimensional low-energy effective Lagrangian for this mode. That is, we integrate the $\delta\phi$ -terms in eq. (3.3) over λ and the coordinates on S^2 and as a result find a four-dimensional action of the form

$$S = -\frac{f_{\pi}^2}{2} \int d^4x \partial_{\mu}(\delta\phi) \partial^{\mu}(\delta\phi), \quad (4.17)$$

where f_π is the pion decay constant. From eq. (3.3), then we have

$$\begin{aligned} f_\pi^2 &= T_{\text{D6}} U_{\text{KK}}^3 \int d\Omega_{\mathcal{S}^2} \sqrt{h} \int_0^\infty d\lambda \lambda^2 \frac{9}{4M_{\text{KK}}^2} \frac{\bar{r}_{\text{vac}}^2}{\bar{\rho}_{\text{vac}}^3} \left(1 + \frac{1}{4\bar{\rho}_{\text{vac}}^3}\right)^{4/3} \sqrt{1 + \bar{r}_{\text{vac}}^2} \\ &= 4\pi T_{\text{D6}} U_{\text{KK}}^3 \int_0^\infty d\lambda \bar{\mu}(\lambda). \end{aligned} \quad (4.18)$$

Combining this result with eqs. (2.24) and (2.29), we see that eq. (4.16) is precisely the GMOR relation (1.2), as anticipated.

We close this section by verifying the agreement between the analytical expression (4.16) above and the results obtained purely by numerical methods and displayed in figure 4a. The integral in equation (4.16) can be evaluated numerically with the result

$$\int_0^\infty d\lambda \bar{\mu}(\lambda) = \frac{9}{4M_{\text{KK}}^2} \int_0^\infty d\lambda \frac{\lambda^2 \bar{r}_{\text{vac}}^2}{\bar{\rho}_{\text{vac}}^3} \left(1 + \frac{1}{4\bar{\rho}_{\text{vac}}^3}\right)^{4/3} \sqrt{1 + \bar{r}_{\text{vac}}^2} \simeq \frac{0.97}{M_{\text{KK}}^2}. \quad (4.19)$$

Similarly, the numerical result for the constant c for zero quark mass (see Figure 2) is $\bar{c} \simeq 0.71$. Substituting these two values in equation (4.16) we get $M^2 \simeq 0.73 M_{\text{KK}}^2 \delta r_\infty$, in exact agreement with a best-fit of the points in figure 4a.

Recall from section 2 that for nonvanishing quark mass we found that there are two possible values of the quark condensate, differing in sign, but that only the negative condensate is stable. In section 3.2 the positive-condensate solution was explicitly shown to be unstable by showing that the pseudo-Goldstone mode δY was tachyonic for this configuration. Since the field-theoretic arguments establishing the GMOR relation apply regardless of the sign of the quark condensate, the squared mass of this mode should also obey the GMOR relation, at least approximately, with an appropriate sign change. Recall that eq. (1.2) represents the first term in an expansion around $m_q = 0$. Now in the string description at $m_q = 0$, the D6-brane configurations for positive and negative c are identical, except for a rotation of ϕ by π . Hence up to a crucial sign, the numerical coefficients in eq. (4.16) are unchanged and hence the tachyonic mode should satisfy $M_Y^2 \simeq -0.73 M_{\text{KK}}^2 \delta r_\infty$. From Figure 5, it does indeed appear that the slopes of the lowest-lying $\delta\phi$ and δY modes are equal, but opposite in sign. More precisely, our best-fit of the numerical results for negative c gave $M_Y^2 \simeq -0.72 M_{\text{KK}}^2 r_\infty$, which gives agreement to within about 1.4%.

5. Multiple flavours ($N_f > 1$) and a holographic Vafa–Witten theorem

Consider a vector-like gauge theory with vanishing θ -angle (like QCD) and N_f flavours, all with identical mass $m_q > 0$. The Vafa–Witten theorem states that the vector-like $U(N_f)$ flavour symmetry cannot be spontaneously broken [19]. This theorem does not exclude the possibility that, at $m_q = 0$, the $U(N_f)$ -preserving vacuum becomes degenerate with one or more $U(N_f)$ -breaking vacua. In this section we discuss the holographic realization of the Vafa–Witten theorem, within the approximations implied by the validity of the supergravity/Born–Infeld theory. In particular, we are considering $N_c \rightarrow \infty$ and $N_f \ll N_c$. Note that, strictly speaking,

the Vafa–Witten theorem need not apply to the gauge theory on the D4/D6-brane system because of the presence of Yukawa-like couplings between the fundamental fermions and the adjoint scalars. However, the latter scalar fields are massive and the theorem should certainly apply in a limit where the scalar masses are sent to infinity. Further, one expects the same result for large but finite masses since the vacuum should still not be sensitive to the scalars. In the present case, the scalar masses are likely of order $M_{\text{KK}} \sim \Lambda_{\text{QCD}}$ and so these couplings would not be suppressed. Hence, from the gauge theory viewpoint, it is not clear a priori whether the effect of these fields can change the vacuum structure to the extent of violating the Vafa–Witten theorem.¹¹ The results of this section answer this question in the negative.

The $U(N_f)$ global symmetry of the gauge theory corresponds, in the string description, to the $U(N_f)$ gauge symmetry on the worldvolume of N_f D6-brane probes in the geometry (2.1). Their dynamics is described by the so-called non-Abelian Dirac–Born–Infeld (DBI) action [23]. This is a generalisation of the single-brane Abelian theory (2.16), in which both the gauge fields and the transverse scalars are promoted to Hermitian, $U(N_f)$ matrices. This means, in particular, that the positions of the D6-branes are no longer commuting quantities in general. In the particular cases in which the transverse scalar matrices can be simultaneously diagonalised, each of their N_f eigenvalues can be interpreted as the position of one of the D6-branes along the corresponding transverse direction.

For the $U(N_f)$ global symmetry to be realized in the gauge theory, the mass matrix for the fundamental quarks must be diagonal with all eigenvalues equal to m_q . In our string picture, this translates into the boundary condition that, asymptotically, all the D6-branes should have the same asymptotic boundary conditions. That is, they are all aligned with each other in the (z^5, \dots, z^9) subspace and all lie at a distance $2\pi\ell_s^2 m_q$ from the origin. We would like to show that the configuration (which obviously satisfies the boundary condition above) in which all the D6-branes are exactly coincident, and are embedded exactly as in the case of a single D6-brane, is the minimum-energy solution of the equations of motion that follow from the non-Abelian DBI action.

To avoid problems with the coordinate singularity at $r = 0$, we adopt the Cartesian coordinates X and Y introduced in section 3.2 to describe the transverse positions of the D6-branes in the $r\phi$ -plane. Then the configuration for the N_f coincident six-branes may be written as:

$$X(\lambda) = r_{\text{vac}}(\lambda) \cdot \mathbb{I} , \quad Y(\lambda) = 0 , \quad \tau = \tau_0 \cdot \mathbb{I} , \quad (5.1)$$

where $r_{\text{vac}}(\lambda)$ is the profile for a single D6-brane determined in section 2 and \mathbb{I} is the $N_f \times N_f$ identity matrix. Since all the transverse scalars commute, there is no ambiguity in the interpretation of this solution as N_f overlapping D6-branes lying along the curve $X(\lambda) = r_{\text{vac}}(\lambda)$.

Let us first argue that this configuration is a stable solution of the non-Abelian DBI equations of motion. We start by expanding the non-Abelian DBI action to quadratic order in fluctuations around the above configuration. Since there is an overall single trace in front

¹¹We thank A. Nelson for a discussion on this point.

of the action, to linear order only variations proportional to the identity generator couple to the $U(1)$ background fields, as given above. Hence the resulting expression for these fields is exactly that obtained from the linear variation of the action for a single D6-brane. It thus follows that the configuration (5.1) is a solution of the non-Abelian equations provided $r_{\text{vac}}(\lambda)$ solves the corresponding Abelian equations.

We further observe that, to quadratic order in fluctuations, the non-Abelian DBI action reduces to the sum of N_f^2 identical copies of the Abelian action, one for each of the N_f^2 independent fluctuations. The reasons for this are two-fold: First, given that the background fields in (5.1) are proportional to the identity, the quadratic fluctuations must again contribute a term in the overall $U(1)$. Second, the difference between the non-Abelian and the Abelian DBI actions consists entirely of terms that involve commutators of fields. Hence, with the given background, the only possible nonvanishing commutators will involve two fluctuations, but such expressions are necessarily $SU(N_f)$ -valued, *i.e.*, traceless. It follows that upon tracing over the gauge indices (and integrating by parts), the quadratic action will take the form

$$\int d^7\sigma \sum_{\alpha=1}^{N_f^2} \delta Z^{i\alpha} \mathcal{O}_{ij} \delta Z^{j\alpha} , \quad (5.2)$$

where $Z^i = X, Y$, α is the gauge index and \mathcal{O}_{ij} is the same operator as appears in the quadratic expansion of the Abelian action. Thus the linearized equations of motion, and hence the spectrum, are just N_f^2 copies of those in the Abelian theory describing a single D6-brane embedding. It follows that the solution (5.1) is stable provided its Abelian analogue is stable, which we know to be the case from the analysis of section 3.

Note that these N_f^2 fluctuations of the D6-branes, which give rise to the N_f^2 copies of the spectrum, are distinct physical excitations and *not* gauge-equivalent: each of them is associated to a different generator of $U(N_f)$, so there is no small $U(N_f)$ gauge transformation (that is, one that tends to the identity at infinity in the 0123-directions) that takes one mode into another. In particular, this implies that in the limit $m_q \rightarrow 0$ there are N_f^2 massless, pseudo-scalar particles! We will come back to this point in the last section.

The arguments presented so far show that (5.1) provides a stable extremum of the non-Abelian DBI action, and therefore a local minimum of the energy of the N_f D6-branes. Strictly speaking, this does not exclude the possibility that there exist other minima. If this was the case, then the true vacuum (or vacua) would be that (or those) with the lowest energy. On physical grounds, however, the existence of these other vacua is unlikely. The reason is as follows. If we ignore the interactions of the D6-branes with each other, then it is clear that (5.1) is the minimum-energy solution amongst those satisfying the boundary conditions described above, since in the absence of interactions each D6-brane must minimise its own energy. If we include open string tree-level interactions by describing the D6-branes' dynamics with the non-Abelian DBI action, then the only obvious configuration that satisfies the appropriate boundary conditions is (5.1), which we have shown to be a stable solution. Inclusion of one-loop (or higher) open string interactions between the D6-branes (such as exchange of

closed strings) would presumably just strengthen the conclusion that (5.1) is the preferred solution. To see this, consider the simple case of $N_f = 2$ D6-branes that overlap with each other asymptotically, but that are slightly misaligned in some small region. Locally, this situation is analogous to that of two planar D6-branes in flat space that are almost but not exactly parallel, in which we know that there is a net force that tends to align the branes. It seems plausible that a similar force will act on the branes in the situation of interest here, and therefore that the preferred configuration will be (5.1), in which all the branes are perfectly aligned with each other.

This conclusion provides a holographic realisation of the Vafa–Witten theorem, since the $U(N_f)$ gauge symmetry on the D6-branes is unbroken if and only if they are all exactly coincident.

By continuity, the arguments above imply that, in the limit $m_q \rightarrow 0$, the $U(N_f)$ -preserving configuration has an energy no greater than that of any other configuration. Just like in the Vafa–Witten theorem, however, this does not rule out the possibility that in this limit some other state becomes degenerate with that in eq. (5.1). In fact, the appearance of N_f^2 massless modes in the linearized spectrum at $m_q = 0$ suggests that the D6-branes might be free to rotate independently in the 89-plane.¹² To see that this is indeed the case, consider, for simplicity, the $N_f = 2$ configuration

$$X(\lambda) = r_{\text{vac}}(\lambda) \cos \phi_0 \cdot \mathbb{I} , \quad Y(\lambda) = r_{\text{vac}}(\lambda) \sin \phi_0 \cdot \sigma_3 , \quad \tau = \tau_0 \cdot \mathbb{I} , \quad (5.3)$$

where $\sigma_3 = \text{diag}(1, -1)$ and ϕ_0 is some fixed angle. The radial vacuum profile above is that corresponding to $r_\infty = 0$. This configuration consists of two D6-branes with the same radial profiles but separated an angle $2\phi_0$ in the 89-plane, and obviously satisfies the boundary condition that the branes overlap at $\lambda \rightarrow \infty$. To see that it solves the non-Abelian equations of motion, consider expanding the non-Abelian DBI action to linear order in fluctuations around (5.3), as before. Since commutator terms are irrelevant at this order, and X and Y are diagonal, the non-Abelian action again reduces to the sum of two identical Abelian actions. In fact, the same argument shows that not only is the configuration (5.3) a solution of the non-Abelian equations, but also that its energy is, for all ϕ_0 , equal to twice that of a single D6-brane. It follows that (5.3) is stable for all ϕ_0 . To see this, suppose that it is not, *i.e.*, that there is some fluctuation around it that is tachyonic. Presumably, this would mean that this solution can decay to another one of lower energy. However, the latter would also have lower energy than the solution with $\phi_0 = 0$, in contradiction with our continuity argument above.

Note that the previous reasoning applies equally well to any distribution of N_f D6-branes around the ϕ -circle, since it only relies on X and Y being diagonal. Thus, at $m_q = 0$, all these configurations are degenerate, lowest-energy, stable solutions. Although it may be an interesting exercise to verify their stability explicitly by expanding the non-Abelian DBI

¹²Note that this is not guaranteed by the existence of massless modes, since this does not exclude the appearance of higher order potential terms for the fluctuations, *e.g.* δZ^4 .

action to quadratic order in fluctuations around (5.3), one should keep in mind that this conclusion is only expected to hold at leading order in the $1/N_c \sim g_s$ expansion, since, as discussed above, we expect higher-order effects to lead to an attractive force between the branes, which would tend to align them.

6. Finite temperature physics

The gauge theory we have so far been describing is at zero temperature. To study the theory at a finite temperature T , we may follow the standard prescription: analytically continue the time coordinate $t \rightarrow t_E = it$, periodically identify t_E with period $\delta t_E = 1/T$, and impose anti-periodic boundary conditions on the fermions around the t_E -circle. This prescription applies equally well in the gauge theory and in the dual string description. In the latter, however, one must consider all possible spacetime solutions with the appropriate boundary conditions, that is, possible saddle points of the Euclidean path integral over supergravity (or rather, string) configurations [2].

In the present case, there are two¹³ Euclidean supergravity solutions which must be considered. The first is simply the Euclideanised version of that appearing in eq. (2.1),

$$ds^2 = \left(\frac{U}{R}\right)^{3/2} \left(dt_E^2 + \sum_{i=1}^3 dx^i dx^i + f(U) d\tau^2\right) + \left(\frac{R}{U}\right)^{3/2} \frac{dU^2}{f(U)} + R^{3/2} U^{1/2} d\Omega_4^2, \quad (6.1)$$

which dominates at low temperatures. Recall that $f = 1 - U_{\text{KK}}^3/U^3$. The second is the Euclidean black hole coming from a nonextremal D4-brane throat

$$ds^2 = \left(\frac{U}{R}\right)^{3/2} \left(\tilde{f}(U) dt_E^2 + \sum_{i=1}^3 dx^i dx^i + d\tau^2\right) + \left(\frac{R}{U}\right)^{3/2} \frac{dU^2}{\tilde{f}(U)} + R^{3/2} U^{1/2} d\Omega_4^2, \quad (6.2)$$

which dominates at high temperatures. In this case, $\tilde{f} = 1 - U_{\text{T}}^3/U^3$. In the Lorentzian-signature solution, the event horizon is located at $U = U_{\text{T}}$.

Of course, these Euclidean metrics are identical up to interchanging the role of t_E and τ (and replacing U_{KK} with U_{T}). To match the boundary conditions set by the finite-temperature gauge theory, we identify these coordinates with periods

$$\delta t_E = \frac{1}{T}, \quad \delta \tau = \frac{2\pi}{M_{\text{KK}}}, \quad (6.3)$$

in both solutions. Since we wish to avoid conical singularities in either spacetime at $U = U_{\text{KK}}, U_{\text{T}}$, the boundary conditions fix the metric parameters as

$$U_{\text{KK}} = \left(\frac{4\pi}{3\delta\tau}\right)^2 R^3, \quad U_{\text{T}} = \left(\frac{4\pi}{3\delta t_E}\right)^2 R^3. \quad (6.4)$$

¹³In analogy with [24], there may be an infinite family of Euclidean solutions labelled by two integers specifying which cycle of the $t_E\tau$ -torus shrinks to zero-size in the bulk. However, given that the t_E - and τ -axes are orthogonal, here either the solutions in eq. (6.1) or (6.2) will dominate the path integral.

As we commented above, the metric (6.1) dominates the path integral at low temperatures, whereas that given by eq. (6.2) dominates at high temperatures. One determines the transition point by comparing the Euclidean action of these two solutions [2]. As the metrics describe the same geometry, it is easy to see that the transition occurs precisely when $\delta\tau = \delta t_E$. That is, a phase transition occurs at the critical temperature

$$T_{\text{deconf}} = M_{\text{KK}}/2\pi. \quad (6.5)$$

From the gauge theory viewpoint, this is a confinement/deconfinement phase transition. This can be seen by the fact that the temporal Wilson loop (around t_E) vanishes for the low-temperature background (6.1), whereas it is nonvanishing for the Euclidean black hole (6.2) [2]. Alternatively, on the Lorentzian sections, the Wilson loop as computed from the solution (2.1) exhibits an area law behaviour, while that computed for the Lorentzian black hole does not because the string can break in two pieces, each having an endpoint at the horizon [26]. One might also observe that, in the low-temperature phase, one has a discrete spectrum of glueballs [3], but this gives way to a continuum of excitations in the high-temperature phase dual to the black hole background.¹⁴ The analogous phase transition in 3+1 dimensions was discussed in ref. [25]. Finally, note that the phase transition takes place at a temperature, (6.5), where the gauge theory is starting to behave five-dimensionally, rather than four-dimensionally.

The preceding discussion refers only to the physics of the (compactified) five-dimensional gauge theory and is independent of the presence of fundamental matter fields. In previous sections we have exhaustively analysed the physics of dynamical quarks in the confining phase. We can extend the discussion to the deconfining phase by considering probe D6-branes in the black hole background (6.2). In reference [14] the study of D7-branes in an asymptotically AdS_5 black hole background revealed the existence of two sets of regular embeddings, parametrised by the quark mass and chiral condensate of the dual gauge theory, and distinguished by whether or not the D7-brane intersects the horizon. It was suggested that the gauge theory undergoes a phase transition, signalled by a discontinuity in dc/dm_q , when the D7-brane undergoes its ‘geometric’ transition. Here we consider similar physics in our four-dimensional gauge theory.

As before, the D6-branes span (Euclidean) time and the spatial 123-directions in common with the D4-brane worldvolume, and lie at a fixed value of τ . In parallel with the steps described by eqs. (2.11–2.14), we introduce isotropic coordinates $\{\lambda, \Omega_2, r, \phi\}$ for the Euclidean black hole (6.2). Furthermore, we rescale to dimensionless coordinates

$$\lambda \rightarrow U_T \lambda, \quad r \rightarrow U_T r, \quad \rho \rightarrow U_T \rho, \quad (6.6)$$

in analogy with eq. (2.18). Now the embedding equation for $r(\lambda)$ becomes

$$\frac{d}{d\lambda} \left[\left(1 - \left(\frac{1}{4\rho^3} \right)^2 \right) \lambda^2 \frac{\dot{r}}{\sqrt{1 + \dot{r}^2}} \right] = \frac{3}{8} \frac{r\lambda^2}{\rho^8} \sqrt{1 + \dot{r}^2}. \quad (6.7)$$

¹⁴Note that the spectrum would again be calculated with Lorentzian signature.

Comparing this result with eq. (2.19), we see that the sign of the right-hand side has changed. As we will see below, this change of sign indicates that the brane now bends towards $U = U_T$: as expected, the black hole exerts an attractive force on the D6-brane, in contrast to the repulsive force in the D4-soliton background.

If we look for asymptotically constant embeddings such that $r(\lambda) \rightarrow r_\infty = L/U_T$ as $\lambda \rightarrow \infty$, we find the same long-distance behaviour as before:

$$r \simeq r_\infty + \frac{c}{\lambda}. \quad (6.8)$$

These asymptotic parameters are related to the quark mass and chiral condensate as before, except for the substitution of U_T for U_{KK} :

$$m_q = \frac{U_T r_\infty}{2\pi\ell_s^2}, \quad \langle \bar{\psi}\psi \rangle = -8\pi^2 \ell_s^2 T_{\text{D6}} U_T^2 c. \quad (6.9)$$

Again, the embedding equation can be solved numerically for any value of r_∞ , with the asymptotic boundary conditions implicit in (6.8). Inspection of the results reveals that, just as in reference [14], two qualitatively different types of profile are possible: those for which the probe brane intersects the horizon, and those for which it does not. As we vary the boundary condition r_∞ , we find that there is a unique embedding for sufficiently large or small values. In the case of small r_∞ , the unique embedding is such that the D6-brane falls into the horizon, whereas in the large- r_∞ case it does not, despite, of course, still being attracted by the black hole. For an intermediate range with $r_\infty \sim 1$, we find that more than one embedding is possible. In particular, for a given r_∞ , we find both embeddings which intersect the horizon and those where the D6-brane smoothly closes off before reaching the horizon. Furthermore, we also find that there are typically multiple solutions of at least one of these varieties of embedding; figure 6 displays some representative examples. These results imply that in varying from large to small r_∞ , there will be a phase transition in the behaviour of the quarks. This transition will occur in the intermediate regime, where, for a fixed temperature and quark mass, the condensate in the gauge theory can have multiple values. Of course, the true ground-state condensate will be selected by minimizing the energy density.

Combining various results — see eqs. (2.6), (6.3), (6.4) and (6.9) — the relation between the temperature and r_∞ is found to be

$$T = \frac{\bar{M}}{\sqrt{r_\infty}}, \quad \text{with } \bar{M}^2 \equiv \frac{9}{4\pi} \frac{m_q M_{\text{KK}}}{g_{\text{YM}}^2 N_c}. \quad (6.10)$$

Here \bar{M} can be interpreted, for a given quark mass, as the typical meson mass scale in the regime where supersymmetry is restored in the zero-temperature gauge theory — see the discussion below eq. (3.16). In the zero-temperature analysis of previous sections we regarded the variation of r_∞ as a variation of the quark mass, while U_{KK} or, equivalently, the KK scale, was fixed. In this section we wish to study the phase structure of the gauge theory as the temperature is varied, keeping the microscopic gauge theory parameters, and in particular

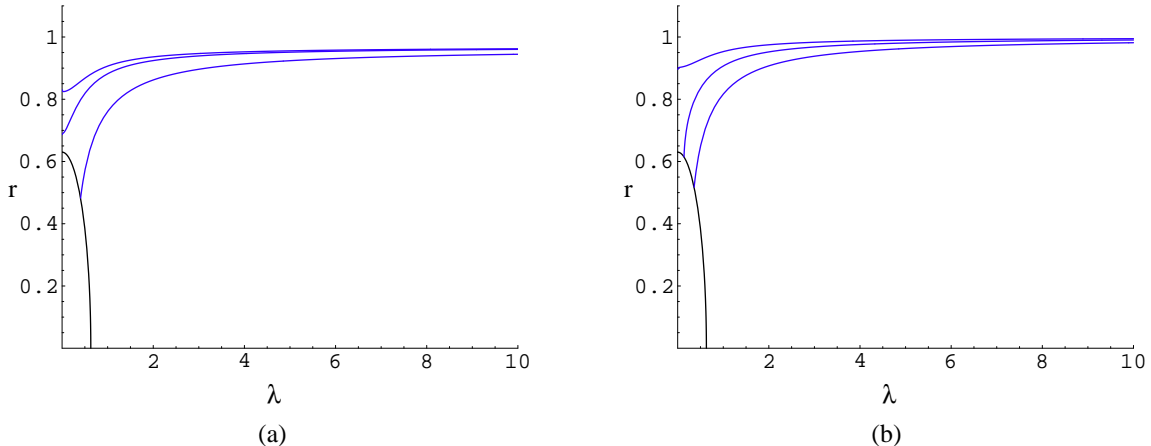


Figure 6: Some representative D6-brane embeddings from the region in which c is multi-valued. The three profiles in each figure have the same asymptotic value of r_∞ ; in (a) two of them avoid the horizon whereas in (b) two fall into the horizon.

the quark mass, fixed. For this reason, since in this phase the physics will only depend on the ratio T/\bar{M} , as suggested by eq. (6.10), we will think of the variation of r_∞ as a variation of the temperature.

The behaviour of the condensate (represented by c) as a function of the temperature is shown in figures 7a and 7b. These plots display some interesting features. First note that $c \rightarrow 0$ both as $T \rightarrow 0$ and as $T \rightarrow \infty$. In the high-temperature regime, the unique embedding is such that the D6-brane falls into the horizon. By following the solid line in the figure, we see that these embeddings only exist down to some minimum temperature, $T \simeq 0.9869\bar{M}$. Similarly there is a unique embedding at sufficiently low temperatures such that the D6-brane does not reach the horizon, and following the dashed line shows that embeddings of this form only exist up to $T \simeq 1.0202\bar{M}$. As shown most clearly in figure 7b, multiple solutions exist in the intermediate temperature range between the two values given above.

Naturally, where more than one solution to the embedding equation exists, the ground-state profile will be that selected out by lowest energy density. Since we are considering static configurations, the energy density is given by

$$\mathcal{E} = - \int d\lambda d\Omega_2 \mathcal{L} = 4\pi T_{\text{D6}} U_{\text{T}}^3 \int_{\lambda_{\text{min}}}^{\infty} d\lambda \left(1 - \left(\frac{1}{4\rho^3} \right)^2 \right) \lambda^2 \sqrt{1 + \dot{r}^2}, \quad (6.11)$$

where λ_{min} is either zero, or the point where the brane meets the horizon, depending on which variety of embedding we are considering. This integral is divergent, so to compare the energy densities of different embeddings we regularize \mathcal{E} by using as a reference the embedding $r(\lambda) = 0$, which runs from the horizon (at $\lambda = \lambda_{\text{H}}$, say) to infinity. Since this is a numerical calculation, we also introduce a cut-off, λ_{match} , in λ at the point where, by imposing the appropriate boundary conditions, we match the numerical profile to the asymptotic solution,

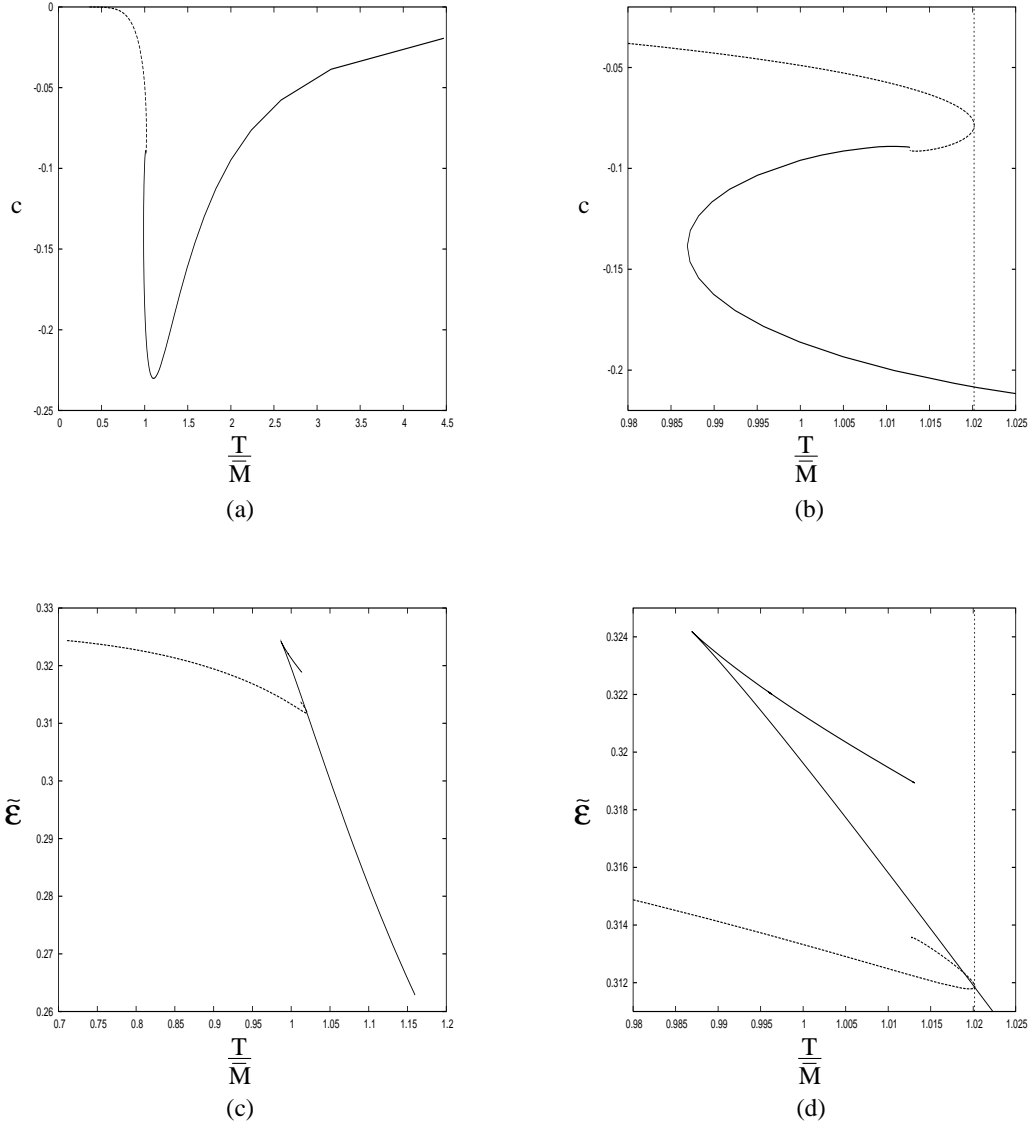


Figure 7: The quark condensate $\langle \bar{\psi}\psi \rangle \propto c$ (plots (a) and (b)), and the energy density $\tilde{\mathcal{E}}$ (plots (c) and (d)) as functions of temperature. The solid (dashed) lines describe the family of embeddings that do (not) intersect the horizon. Plots (b) and (d) show in more detail the regions of plots (a) and (c) where the two branches intersect. The vertical line lies at $T = T_{\text{fund}}$, the temperature at which the phase transition in the behaviour of the quarks takes place.

$r \simeq r_\infty + c/\lambda$. There is an infinite contribution to \mathcal{E} from the remainder of the profile, but when regularized the leading behaviour of this correction can be shown to be

$$\mathcal{E}_{\text{corr}} = \frac{c^2}{2\lambda_{\text{match}}} + \mathcal{O}(\lambda_{\text{match}}^{-3}). \quad (6.12)$$

Therefore, to be precise, we compare the energy densities by calculating

$$\tilde{\mathcal{E}} = \frac{\mathcal{E}_{\text{reg}}}{4\pi T_{\text{D6}} U_{\text{T}}^3} \equiv \int_{\lambda_{\text{min}}}^{\lambda_{\text{match}}} d\lambda \left(1 - \left(\frac{1}{4\rho^3} \right)^2 \right) \lambda^2 \sqrt{1 + \dot{r}^2} - \int_{\lambda_{\text{H}}}^{\lambda_{\text{match}}} d\lambda \left(\lambda^2 - \frac{1}{16\lambda^4} \right) + \frac{c^2}{2\lambda_{\text{match}}}. \quad (6.13)$$

We then trust that this provides a valid basis for the comparison of different energy densities when the differences in $\tilde{\mathcal{E}}$ are greater than $\mathcal{O}(\lambda_{\text{match}}^{-3})$. This is the case here, as we use $\lambda_{\text{match}} = 100$.

The energy density $\tilde{\mathcal{E}}$ is plotted as a function of temperature in figures 7c and 7d. Starting from low temperatures, figure 7d shows that, as T is increased to that in the intermediate region, the physical embedding remains that which does not reach the horizon. At $T \simeq 1.0202\bar{M}$, the energy density for this embedding and that which falls into the horizon match. For $T > 1.0202\bar{M}$, the energetically favoured embedding is one which falls into the horizon. Therefore, at

$$T \equiv T_{\text{fund}} \simeq 1.0202\bar{M}, \quad (6.14)$$

there is a phase transition in the behaviour of the fundamental quarks. This phase transition is signalled by a discontinuity in $\langle \bar{\psi}\psi \rangle(T)$, as shown in Figure 7b, as well as a discontinuity in the specific heat $d\tilde{\mathcal{E}}(T)/dT$, as can be seen in Figure 7d. Note that, to within the precision of our numerical calculations, T_{fund} cannot be distinguished from the maximum temperature for which a horizon-avoiding embedding is possible.

From the string description with the D4 throat geometry, the basic physics behind this transition is straightforward. Increasing the temperature increases both the radial position of the horizon and energy density of the black hole. For small enough a temperature, the D6-brane is pulled towards the horizon but its tension balances the gravitational attraction. However, above the critical temperature T_{fund} , the gravitational force has increased to the point where it overcomes the tension and the brane is drawn into the horizon.

Another feature that characterizes the present phase transition is that the meson spectrum changes at $T = T_{\text{fund}}$. The discrete spectrum of mesons of the low-temperature phase becomes a continuum of excitations in the high-temperature phase where the D6-brane embedding extends to the horizon. This behaviour is similar to that of the glueball spectrum at the deconfinement phase transition in the gauge theory, discussed previously. Note, however, that for temperatures above T_{deconf} we are, by assumption, in the deconfined phase of the gauge theory, and so it is possible to introduce free quarks; these correspond to open strings extending from the D6-brane down to the horizon. If $T_{\text{deconf}} < T_{\text{fund}}$ there is then a range of temperatures, $T_{\text{deconf}} < T < T_{\text{fund}}$, in which there are free quarks but also a finite mass gap, $m_{\text{eff}}(T) > 0$, associated with the introduction of such quarks into the system. In this regime, there still exists a (discrete) spectrum of bound states with $M < 2m_{\text{eff}}$. Note also that the deconfined adjoint degrees of freedom still generate a finite screening length beyond which the force between a quark and an anti-quark vanishes [26]; in the string description

this happens because the string that joins the quarks together snaps into two pieces, each of them going from the brane to the horizon, that can be separated with no cost in energy. Above T_{fund} , however, $m_{\text{eff}}(T) = 0$ and the spectrum of fundamental matter field excitations becomes continuous.

Up to this point, we have discussed two independent phase transitions: the deconfining phase transition at $T = T_{\text{deconf}}$, for which the holographic dual description involved a discrete change of the bulk spacetime geometry, and the quark phase transition at $T = T_{\text{fund}}$, for which the holographic description involved a discrete jump in the embedding geometry of the D6-brane. However, if the latter is to be realized as a separate phase transition, then it must be true that $T_{\text{fund}} > T_{\text{deconf}}$.¹⁵ In terms of the microscopic parameters, this condition translates into

$$m_q > \frac{0.98}{9\pi} g_{\text{YM}}^2 N_c M_{\text{KK}} . \quad (6.15)$$

In the zero-temperature theory, this is roughly the quark mass scale at which supersymmetry is restored — see the discussion below eq. (3.16).

If $T_{\text{fund}} < T_{\text{deconf}}$, the relevant spacetime geometry at $T = T_{\text{fund}}$ is the D4-soliton (6.1) and the ambiguity in the D6-brane embedding discussed above is not relevant. Alternatively, the gauge theory is still in a confined phase and so the chemical potential to introduce a free quark remains infinite; in the dual description this is because, since there is no horizon, an open string must have both ends on the D6-brane, and so represents a quark/anti-quark bound state. In this case, the two phase transitions are realized simultaneously at $T = T_{\text{deconf}}$. An important example of this behaviour is when $m_q = 0$. In this case, the low-temperature phase is characterized by spontaneous chiral symmetry breaking, as in section 2. In the high-temperature phase, $m_q \rightarrow 0$ is equivalent to $T \rightarrow \infty$ (see eq. (6.10)), in which limit the chiral condensate vanishes (see figure 7a). Hence the deconfining phase transition is also accompanied by the restoration of chiral symmetry in this model.

To close the section, we wish to stress to the reader that while these phase transitions are of inherent interest in understanding the model under study here, they take place in a temperature regime where the gauge theory is intrinsically five-dimensional, rather than behaving in a four-dimensional way, as can be seen by comparing the transition temperatures given in eqs. (6.5) and (6.15) to the compactification scale M_{KK} .

7. D4/D6/ $\overline{\text{D6}}$ -intersections

In the discussion of embeddings in section 2, we noted that the solution $r(\lambda) = 0$ of eq. (2.19) is not a physical one (for $U_{\text{KK}} \neq 0$) if it terminates at the origin of the $U\tau$ -plane because it would correspond to an open D6-brane. However, this solution can be extended through this point to construct a physically acceptable embedding. To see this, recall that the full

¹⁵Note that, in this regime, the fundamental fields still ‘feel’ the deconfining transition at $T = T_{\text{deconf}}$. For example, there is a discontinuity in the chiral condensate $\langle \bar{\psi}\psi \rangle$, which jumps from a negative to a positive value at this phase transition.

D6-brane embedding is further specified by the conditions $\phi = \phi_0$ and $\tau = \tau_0$, where ϕ_0 and τ_0 are arbitrary constants. We can therefore join together a solution with $\tau = \tau_0$ to another one with $\tau = \tau_0 + \delta\tau/2$ (see eq. (2.3)) to obtain a complete regular solution that describes a D6-brane whose projection on the $U\tau$ -plane is a straight line that passes through the origin and intersects the boundary at two antipodal values of τ . This means that this solution describes an intersection of N_c D4-branes with two D6-branes, or, more precisely, with one D6-brane and one anti-D6-brane.¹⁶ Note that these embeddings bear a striking resemblance to those discussed in [13]. The parallel includes the facts that both constructions involve two boundary defects and both preserve the chiral symmetry.

To better understand the defect theory corresponding to these D4/D6/ $\overline{\text{D6}}$ -intersections, we consider a family of more general embeddings that describe D6-branes that lie at $r = 0$ (or alternatively, $z^8 = 0 = z^9$) and stretch along some curve $U = U(\tau)$ in the $U\tau$ -plane, intersecting the boundary at two, not necessarily antipodal, values of τ . Such D6-branes wrap a maximal S^2 within the S^4 in the metric (2.1), so the induced metric on their worldvolume is

$$ds^2(g) = \left(\frac{U}{R}\right)^{3/2} \eta_{\mu\nu} dx^\mu dx^\nu + R^{3/2} U^{1/2} d\Omega_2^2 + \left[\left(\frac{U}{R}\right)^{3/2} f(U) + \frac{U'^2}{\left(\frac{U}{R}\right)^{3/2} f(U)} \right] d\tau^2. \quad (7.1)$$

Since the Lagrangian density on the D6-brane

$$\mathcal{L}_{\text{D6}} = -\frac{1}{(2\pi)^6 \ell_s^7} e^{-\phi} \sqrt{-\det g_{\text{ind}}} = T_{\text{D6}} U^2 \sqrt{\left(\frac{U}{R}\right)^3 f(U) + \frac{U'^2}{f(U)}} \quad (7.2)$$

(where $U' = dU/d\tau$) does not depend explicitly on τ , it follows that

$$U' \frac{\partial \mathcal{L}}{\partial U'} - \mathcal{L} = \frac{U^2 \left(\frac{U}{R}\right)^3 f(U)}{\sqrt{\left(\frac{U}{R}\right)^3 f(U) + \frac{U'^2}{f(U)}}} \quad (7.3)$$

is also τ -independent. Let $U_0 \geq U_{\text{KK}}$ be the minimum value of $U(\tau)$. By symmetry we can assume that this value is reached at $\tau = 0$, that is, that we have $U(0) = U_0$ and $U'(0) = 0$. Integrating the equation above we then find

$$\tilde{\tau}(u) = \frac{3}{2} b^{7/2} g^{1/2}(b) \int_b^u dx \frac{1}{x^{3/2} g(x) \sqrt{x^7 g(x) - b^7 g(b)}}, \quad (7.4)$$

where we have introduced

$$\tilde{\tau} \equiv \frac{3}{2} \frac{U_{\text{KK}}^{1/2}}{R^{3/2}} \tau, \quad u \equiv \frac{U}{U_{\text{KK}}}, \quad b \equiv \frac{U_0}{U_{\text{KK}}} \geq 1, \quad g(x) \equiv 1 - \frac{1}{x^3}. \quad (7.5)$$

Note that the rescaled angle $\tilde{\tau}$ has period 2π . Eq. (7.4) specifies the D6-brane profile in the $U\tau$ -plane. The D6-brane intersects the boundary at $\tilde{\tau}_\pm(b) = \pm\tilde{\tau}(u \rightarrow \infty)$. These two

¹⁶Technically, the reason is that the orientations on the intersections of the D6-brane with the boundary at $\tau = \tau_0$ and $\tau = \tau_0 + \delta\tau/2$, induced from a given orientation on the D6-brane, are opposite to each other.

points are implicitly fixed by U_0 , the ‘lowest’ point of the D6-brane in the $U\tau$ -plane. In particular, their separation is a monotonically decreasing function of b . It is easy to show that $\tilde{\tau}_{\pm}(b \rightarrow 1) = \pm\pi/2$, so the two points become antipodal as the lowest point of the D6-brane approaches the origin of the $U\tau$ -plane. In this limit the projection of the D6-brane on this plane is just a straight line, as discussed above. In the opposite limit in which the (lowest point of) D6-brane approaches the boundary, the separation between the intersection points becomes smaller and smaller. In the strict limit $b \rightarrow \infty$ the two coincide and the D6-brane disappears.

Now, these embeddings seem to portend fascinating physics for the dual five-dimensional gauge theory coupled to two defects or, more precisely, to a defect and an anti-defect. It appears, however, that this physics is intrinsically five-dimensional. Since the focus of the present paper is the four-dimensional QCD-like physics of the original model, we have not fully explored this system. However, we offer some preliminary remarks in the following.

The deflection of the D6-brane in the τ -direction, which corresponds to a worldvolume direction of the D4-branes, is reminiscent of certain D5-brane embeddings in AdS_5 studied in ref. [27]. These authors found (non-supersymmetric) embeddings in which the D5-brane began at large radius running along r , but were deflected to run parallel to the AdS_5 horizon at some finite radius. At large r , these configurations can be understood as D3/D5 intersections that are T-dual to that represented in (1.1). The dual gauge theory involved coupling $\mathcal{N} = 4$ SYM to a $(2 + 1)$ -dimensional defect which broke all supersymmetries. The deflection was interpreted as giving an expectation value to an operator in the defect theory.

In the present case, the D4-soliton background breaks the supersymmetry but with both defects, supersymmetry would still not be restored in the limit $U_{\text{KK}} \rightarrow 0$;¹⁷ one way to understand this in the field theory is to note that the half of the supersymmetries of the ambient theory preserved (broken) by the defect are precisely those that are broken (preserved) by the anti-defect.¹⁸ The embeddings described by eq. (7.4) would correspond to a state where a symmetric pair of operators in each defect theory simultaneously acquire identical expectation values. Indirectly, the D6-brane embedding would also induce different expectation values of gauge theory operators, *e.g.*, $\text{Tr } F^2$, in the two regions on the τ -circle divided by the defects.

At the microscopic level, there are two sets of fundamental matter fields in the field theory, one associated with each defect. This is realised in the string description by the fact that, despite there being a single D6-brane, its intersection with a constant- $U > U_0$ slice consists of two disconnected pieces, corresponding to two independent sets of active degrees of freedom at the corresponding energy scale. These degrees of freedom seem to disappear for energy scales associated to radial positions $U < U_0$, as in [27]. As discussed above, the D6-brane disappears in the limit $\tilde{\tau}_+ - \tilde{\tau}_- \rightarrow 0$. Consistently, in this limit $U_0 \rightarrow \infty$ and the degrees of freedom above are completely removed. In the gauge theory, this corresponds to the limit in which the defect and the anti-defect are brought on top of each other.

¹⁷Note that the supersymmetry breaking of the background is not essential to constructing the general embeddings, *i.e.*, one can simply replace $g(x)$ by 1 everywhere in eq. (7.4).

¹⁸Defect/anti-defect configurations, and more general multiple defect configurations, were discussed in [28].

This situation may be compared with that where both defects are associated with a ‘standard’ D6-brane embedding as described in section 2; one at $\tilde{\tau} = \tilde{\tau}_+$ and the other at $\tilde{\tau} = \tilde{\tau}_-$. Of course, in this case there are also two sets of independent degrees of freedom associated with open string excitations on both the D6- and $\overline{\text{D6}}$ -brane.¹⁹ However, one difference is that the spectrum of these excitations will now be independent of the defect/anti-defect separation, $\tilde{\tau}_+ - \tilde{\tau}_-$.²⁰ In addition, one would also find excitations corresponding to open strings stretching between the two separate branes. In contrast, in the case of a single D6-brane, the two defects can interact through open string modes that propagate along the brane from one defect to the other.

Of course, one should ask the question which embedding minimizes the energy density of the system. That is, does energetics favour the smooth embedding which joins the two boundary defects or that in which there are two independent branes? As a preliminary step in this direction, we compared the energy density for the ‘standard’ embeddings of the D6- and $\overline{\text{D6}}$ -brane pair with $r_\infty = 0$ to that of the smooth embedding above with $U_0 = U_{\text{KK}}$ (and hence $\tilde{\tau}_+ - \tilde{\tau}_- = \pi$). Our numerical results indicate that the smooth embedding produces a lower energy density and hence describes the true vacuum configuration. Note then that with both defects corresponding to the D6- and $\overline{\text{D6}}$ -branes, the vacuum preserves chiral symmetry.

Presumably if U_0 is increased above U_{KK} , the smooth embeddings described above would continue to be energetically favored as it seems the energy density for these solutions must decrease as $\tilde{\tau}_+ - \tilde{\tau}_-$ decreases while that for the standard embeddings remains unchanged. Note, however, that the above are just two particular cases of a more general family of embeddings in which the brane bends simultaneously in the 89- and the $U\tau$ -planes, that is, embeddings with nontrivial functions $r = r(\lambda)$ and $\tau = \tau(\lambda)$ (using the notation of section 2). In general, we expect the minimum-energy two-defect embedding is of this type.

These defect theories might be explored in other ways as well. For example, one might also consider varying the parameter ρ_∞ for the two defects, which may be done independently for each of the defects. Finally, of course, one might also consider the effects of a finite temperature, as in section 6.

8. Discussion

We have analyzed in detail the case of a single D6-brane, which corresponds to a single flavour in the gauge theory. In this case the gauge theory enjoys (at large N_c) an exact $U(1)_V \times U(1)_A$ symmetry. The first factor is just the flavour symmetry, which in the string description corresponds to the gauge symmetry on the worldvolume of the D6-brane. The second factor is a chiral symmetry that rotates the left- and right-handed fermions, ψ_L and ψ_R , with opposite phases; it also rotates by a phase the adjoint scalar $X = X^8 + iX^9$, as is

¹⁹Note that in this case one may also realise a defect/defect (as opposed to a defect/anti-defect) theory by considering two D6-branes.

²⁰In the approximation in which interactions between the branes, which are suppressed in the large- N_c limit, are neglected.

clear from the fact that in the string description the $U(1)_A$ symmetry is just the rotational symmetry in the 89-plane.

Like in QCD, we expect the $U(1)_A$ symmetry to be spontaneously broken by a chiral condensate, $\langle \bar{\psi}\psi \rangle \neq 0$, and hence the existence of the corresponding Goldstone boson in the spectrum; this is the analog of the QCD η' particle (which is massless in the $N_c \rightarrow \infty$ limit), but, in an abuse of language, we have referred to it as a ‘pion’. The string description indeed confirms the field theory expectation: for zero quark mass, there is precisely one massless pseudo-scalar (in the four-dimensional sense) fluctuation of the D6-brane. If $m_q > 0$ this pion becomes a pseudo-Goldstone boson. Its mass, as well as the chiral condensate and the pion decay constant, can be computed in the string description, and we have shown that these three quantities and the quark mass obey the Gell-Mann–Oakes–Renner relation (1.2) [18]. Although this is a reassuring result, one should keep in mind that, just like in field theory, it is essentially a consequence of the *symmetry*-breaking pattern.

In the case $N_f > 1$ we provided a holographic version of the Vafa–Witten theorem, which states that, in a vector-like theory with zero θ -angle (like QCD) and N_f quark flavours of identical masses $m_q > 0$, the global, $U(N_f)$ flavour symmetry cannot be spontaneously broken. As we discussed, it is a priori unclear, on field theory grounds, that the Vafa–Witten theorem does apply to the actual gauge theory on the D4-branes, because of the presence of Yukawa-like couplings to scalar fields of masses $M_{\text{KK}} \sim \Lambda_{\text{QCD}}$. The result from the string analysis therefore established that the presence of these fields does not alter the vacuum structure of the theory to the extent of violating the Vafa–Witten theorem.

The global $U(N_f)$ symmetry of the gauge theory becomes the gauge symmetry on the worldvolume of N_f D6-branes in the string description. The holographic version of the Vafa–Witten theorem is the statement that the minimum-energy configuration for the N_f D6-branes is a $U(N_f)$ -preserving one in which all branes lie on top of each other. It should be emphasised that, unlike the Gell-Mann–Oakes–Renner relation, the Vafa–Witten theorem is not based on a symmetry(-breaking) argument, but depends on the *dynamics* of the theory. In the field theory, the proof relies on the reality and positivity of the fermion determinant that arises in the path integral formulation; in the holographic version, it relies on details of the dynamics of multiple D6-branes.

One result of our analysis of the $N_f > 1$ case is the existence of N_f^2 independent, massless fluctuations of the D6-branes if $m_q = 0$. It is tempting to interpret the associated N_f^2 massless pseudo-scalar particles in the spectrum of the gauge theory as the Goldstone bosons of a spontaneously broken $U(N_f)_A$ symmetry, to which the $U(1)_A$ symmetry would putatively be enhanced for $N_f > 1$. However, only one of the N_f^2 states above is a true Goldstone boson, for two reasons. First, the five-dimensional theory contains a term of the form $\bar{\psi}_i X \psi^i$, where $i = 1, \dots, N_f$ is the flavour index. Since X only transforms under the $U(1)_A$ subgroup of $U(N_f)_A$, the theory is only invariant under $U(1)_A \times U(N_f)_V$, which is spontaneously broken to $U(N_f)_V$. Although X is a massive field that can be integrated out, its mass $M_X \sim M_{\text{KK}} \sim \Lambda_{\text{QCD}}$ is of the same order as the strong coupling scale, so its integration should not lead to a real suppression of the symmetry-breaking operator above.

The second reason that makes implausible the interpretation of all but one of the massless modes above as Goldstone bosons is that they have non-derivative interactions. Indeed, the effective, interacting Lagrangian for these modes is obtained by expanding the non-Abelian Dirac–Born–Infeld action for the N_f D6-branes [23] beyond quadratic order and then dimensionally reducing it to four dimensions, as we did in Section 4 in the $N_f = 1$ case. Since the action for the D6-branes contains non-derivative interactions, such as commutator terms squared, so does the effective four-dimensional Lagrangian. These terms are only absent for the mode that multiplies the identity generator of $U(N_f)$. The caveat as to why this argument makes the Goldstone boson interpretation for the other modes implausible, but not strictly impossible, is that the coefficients in the effective Lagrangian might conspire so that, once all contributing diagrams are included, only momentum-dependent parts survive in any scattering amplitude (as in the linear sigma-model for the pion Lagrangian [29]). This possibility seems rather unlikely.

Thus we conclude that the string description predicts the existence of N_f^2 massless pseudo-scalar particles in the spectrum of the quantum gauge theory in the large- N_c limit. Once sub-leading effects in the $1/N_c$ expansion are included, we expect these particles to acquire a small mass. The $U(1)_A$ symmetry is anomalous at finite N_c , so its associated Goldstone boson is not exactly massless at finite N_c ; presumably, this anomaly can be analysed in the supergravity description along the lines of [6, 30, 31, 32]. The other $N_f^2 - 1$ modes are likely to acquire a mass due to closed string interactions between the D6-branes, which are a $g_s \sim 1/N_c$ effect. From the gauge theory viewpoint, we have found no obvious reason for the masslessness (or lightness, at finite N_c) of these $N_f^2 - 1$ pseudo-scalars, since we have argued that they are not Goldstone bosons.²¹ Recall that, from the string viewpoint, the reason for this is that the only difference between the non-Abelian and the Abelian DBI actions consists exclusively of terms that involve commutators of fields. This can be regarded as a consequence of the fact that the seven-dimensional D6-brane action is T-dual to the ten-dimensional action of D9-branes; all commutators of scalar fields in the D6-brane action originate from commutators of gauge fields in the non-Abelian field strength on the D9-branes. Thus, it is *ten*-dimensional $U(N_f)$ gauge invariance that seems to be responsible, from the string viewpoint, for the lightness of the gauge theory scalars.²² Given the importance in high energy physics of mechanisms that naturally allow small scalar masses, it would be interesting to understand how to rephrase the constraints imposed by ten-dimensional $U(N_f)$ gauge invariance purely in four-dimensional field theory terms.

Acknowledgments

We are especially grateful to J. Brodie for helpful conversations. We also wish to thank J. Donoghue, J. Erdmenger, J. I. Latorre, A. E. Nelson, D. T. Son, M. J. Strassler, S. Thomas, D. Tong and A. Uranga for discussions and comments. Research at the Perimeter Institute is

²¹Other examples with ‘unexpectedly’ light scalars in the context of AdS/CFT have been discussed in [33].

²²This observation is due to M. Strassler.

supported in part by funds from NSERC of Canada. RCM is further supported by an NSERC Discovery grant, DJW by Fonds FCAR du Québec and by a McGill Major Fellowship, while MK is supported in part by NSF grants PHY-0331516, PHY99-73935 and DOE grant DE-FG02-92ER40706. DJW wishes to thank the University of Waterloo Physics Department for their ongoing hospitality and MK would like to thank the Perimeter Institute for Theoretical Physics for partial support and hospitality while this work was being performed.

References

- [1] J. M. Maldacena, *The large N limit of superconformal field theories and supergravity*, *Adv. Theor. Math. Phys.* **2** (1998) 231 [*Int. J. Theor. Phys.* **38** (1998) 1113], [hep-th/9711200](#).
- [2] E. Witten, *Anti-de Sitter space, thermal phase transition, and confinement in gauge theories*, *Adv. Theor. Math. Phys.* **2** (1998) 505, [hep-th/9803131](#).
- [3] C. Csaki, H. Ooguri, Y. Oz and J. Terning, *Glueball mass spectrum from supergravity*, *J. High Energy Phys.* **01** (1999) 017, [hep-th/9806021](#); R. de Mello Koch, A. Jevicki, M. Mihailescu and J. P. Nunes, *Evaluation of glueball masses from supergravity*, *Phys. Rev.* **D 58** (1998) 105009, [hep-th/9806125](#); H. Ooguri, H. Robins and J. Tannenhauser, *Glueballs and their Kaluza-Klein cousins*, *Phys. Lett.* **B 437** (1998) 77, [hep-th/9806171](#); J. A. Minahan, *Glueball mass spectra and other issues for supergravity duals of QCD models*, *J. High Energy Phys.* **01** (1999) 020, [hep-th/9811156](#); N. R. Constable and R. C. Myers, *Spin-two glueballs, positive energy theorems and the AdS/CFT correspondence*, *J. High Energy Phys.* **10** (1999) 037, [hep-th/9908175](#); R. C. Brower, S. D. Mathur and C. Tan, *Glueball spectrum for QCD from AdS supergravity duality*, *Nucl. Phys.* **B 587** (2000) 249, [hep-th/0003115](#).
- [4] O. Aharony, A. Fayyazuddin and J. M. Maldacena, *The large- N limit of $\mathcal{N} = 2, 1$ field theories from threebranes in F-theory*, *J. High Energy Phys.* **07** (1998) 013, [hep-th/9806159](#).
- [5] A. Karch and L. Randall, *Open and closed string interpretation of SUSY CFT's on branes with boundaries*, *J. High Energy Phys.* **06** (2001) 063, [hep-th/0105132](#).
- [6] M. Bertolini, P. Di Vecchia, M. Frau, A. Lerda, and R. Marotta, *$N=2$ Gauge theories on systems of fractional D3/D7 branes*, *Nucl. Phys.* **B 621** (2002) 157, [hep-th/0107057](#).
- [7] M. Bertolini, P. Di Vecchia, G. Ferretti, and R. Marotta, *Fractional Branes and $N=1$ Gauge Theories*, *Nucl. Phys.* **B 630** (2002) 222, [hep-th/0112187](#).
- [8] A. Karch and E. Katz, *Adding flavor to AdS/CFT*, *J. High Energy Phys.* **06** (2002) 043, [hep-th/0205236](#).
- [9] A. Karch, E. Katz and N. Weiner, *Hadron masses and screening from AdS Wilson loops*, *Phys. Rev. Lett.* **90** (2003) 091601, [hep-th/0211107](#).
- [10] X. J. Wang and S. Hu, *Intersecting branes and adding flavors to the Maldacena-Nunez background*, *J. High Energy Phys.* **09** (2003) 017, [hep-th/0307218](#).
- [11] P. Ouyang, *Holomorphic D7-branes and flavored $N = 1$ gauge theories*, [hep-th/0311084](#).
- [12] M. Kruczenski, D. Mateos, R. C. Myers and D. J. Winters, *Meson spectroscopy in AdS/CFT with flavour*, *J. High Energy Phys.* **07** (2003) 049, [hep-th/0304032](#).

- [13] T. Sakai and J. Sonnenschein, *Probing flavored mesons of confining gauge theories by supergravity*, *J. High Energy Phys.* **09** (2003) 047, [hep-th/0305049](#).
- [14] J. Babington, J. Erdmenger, N. Evans, Z. Guralnik and I. Kirsch, *Chiral symmetry breaking and pions in non-supersymmetric gauge/gravity duals*, [hep-th/0306018](#).
- [15] C. Nunez, A. Paredes and A. V. Ramallo, *Flavoring the gravity dual of $\mathcal{N} = 1$ Yang-Mills with probes*, *J. High Energy Phys.* **12** (2003) 024, [hep-th/0311201](#).
- [16] N. Itzhaki, J. M. Maldacena, J. Sonnenschein and S. Yankielowicz, *Supergravity and the large N limit of theories with sixteen supercharges*, *Phys. Rev.* **D 58** (1998) 046004, [hep-th/9802042](#).
- [17] O. DeWolfe, D. Z. Freedman and H. Ooguri, *Holography and Defect Conformal Field Theories*, *Phys. Rev.* **D 66** (2002) 025009, [hep-th/0111135](#).
- [18] M. Gell-Mann, R. J. Oakes and B. Renner, *Behavior of current divergences under $SU(3) \times SU(3)$* , *Phys. Rev.* **175** (1968) 2195.
- [19] C. Vafa and E. Witten, *Restrictions on symmetry breaking in vector-like gauge theories*, *Nucl. Phys.* **B 234** (1984) 173.
- [20] M. A. Shifman, A. I. Vainshtein and V. I. Zakharov, *QCD and resonance physics. Sum rules.*, *Nucl. Phys.* **B 147** (1979) 385.
- [21] G. T. Horowitz and R. C. Myers, *The AdS/CFT correspondence and a new positive energy conjecture for general relativity*, *Phys. Rev.* **D 59** (1999) 026005, [hep-th/9808079](#).
- [22] U. H. Danielsson, E. Keski-Vakkuri and M. Kruczenski, *Vacua, propagators, and holographic probes in AdS/CFT*, *JHEP* **9901** (1999) 002, [hep-th/9812007](#).
- [23] R. C. Myers, *Dielectric-Branes*, *J. High Energy Phys.* **12** (1999) 022, [hep-th/9910053](#).
- [24] R. Dijkgraaf, J. M. Maldacena, G. W. Moore and E. Verlinde, *A black hole farey tail*, [hep-th/0005003](#).
- [25] R. C. Myers, *Stress tensors and Casimir energies in the AdS/CFT correspondence*, *Phys. Rev.* **D 60** (1999) 046002, [hep-th/9903203](#); S. Surya, K. Schleich and D. M. Witt, *Phase transitions for flat adS black holes*, *Phys. Rev. Lett.* **86** (2001) 5231, [hep-th/0101134](#).
- [26] S. J. Rey, S. Theisen and J. T. Yee, *Wilson-Polyakov loop at finite temperature in large N gauge theory and anti-de Sitter supergravity*, *Nucl. Phys.* **B 527** (1998) 171, [hep-th/9803135](#).
- [27] K. Skenderis and M. Taylor, *Branes in AdS and pp-wave spacetimes*, *J. High Energy Phys.* **06** (2002) 025, [hep-th/0204054](#).
- [28] D. Mateos, S. Ng and P. K. Townsend, *Supersymmetric Defect Expansion in CFT from AdS Supertubes*, *J. High Energy Phys.* **07** (2002) 048, [hep-th/0207136](#).
- [29] J. F. Donoghue, E. Golowich and B. R. Holstein, *Dynamics of the standard model*, Cambridge University Press, 1992.
- [30] I. R. Klebanov, P. Ouyang and E. Witten, *A gravity dual of the chiral anomaly*, *Phys. Rev.* **D 65** (2002) 105007, [hep-th/0202056](#).
- [31] M. Bertolini, P. Di Vecchia, M. Frau, A. Lerda and R. Marotta, *More Anomalies from Fractional Branes*, *Phys. Lett.* **B 540** (2002) 104, [hep-th/0202195](#).

- [32] U. Gursoy, S. A. Hartnoll and R. Portugues, *The chiral anomaly from M theory*,
hep-th/0311088.
- [33] M. J. Strassler, *Non-supersymmetric theories with light scalar fields and large hierarchies*,
hep-th/0309122.